

**ผลของ Echo Time, Echo train length และ Flip angle ใน chemical shift artifact ใน T2  
weighted โดยเทคนิค turbo spin echo pulse sequence**

**นาย ธีรพงศ์ ด้านชนวัฒน์**

**วิทยานิพนธ์นี้เป็นส่วนหนึ่งของการศึกษาตามหลักสูตรปริญญาวิทยาศาสตรมหาบัณฑิต  
สาขาวิชา วิทยาศาสตร์ ภาควิชา รังสีวิทยา  
คณะแพทยศาสตร์ จุฬาลงกรณ์มหาวิทยาลัย  
ปีการศึกษา 2555  
ลิขสิทธิ์ของจุฬาลงกรณ์มหาวิทยาลัย**

บทคัดย่อและแฟ้มข้อมูลฉบับเต็มของวิทยานิพนธ์ตั้งแต่ปีการศึกษา 2554 ที่ให้บริการในคลังปัญญาจุฬาฯ (CUIR)  
เป็นแฟ้มข้อมูลของนิสิตเจ้าของวิทยานิพนธ์ที่ส่งผ่านทางบัณฑิตวิทยาลัย

The abstract and full text of theses from the academic year 2011 in Chulalongkorn University Intellectual Repository (CUIR)  
are the thesis authors' files submitted through the Graduate School.

**EFFECT OF ECHO TIME, ECHO TRAIN LENGTH AND FLIP ANGLE OF T2 WEIGHTED  
TURBO SPIN ECHO IN REDUCTION CHEMICAL SHIFT ARTIFACT**

**Mr. Nuttapong Danthanavat**

**A Thesis Submitted in Partial Fulfillment of the Requirements  
for the Degree of Master of Science Program in Medical Imaging**

**Department of Radiology**

**Faculty of Medicine**

**Chulalongkorn University**

**Academic Year 2012**

**Copyright of Chulalongkorn University**

Thesis Title                    EFFECT OF ECHO TIME, ECHO TRAIN  
                                          LENGTH AND FLIP ANGLE OF T2  
                                          WEIGHTED TURBO SPIN ECHO IN  
                                          REDUCTION CHEMICAL SHIFT ARTIFACT

By                                    Mr.Nuttapong Danthanavat

Field of Study                    Medical Imaging

Thesis Advisor                 Associate Professor Anchali Krisanachinda, Ph.D.

Thesis Co-advisor             Associate Professor Sukalaya Lerdlum, M.D.

---

Accepted by the Faculty of Medicine, Chulalongkorn University in  
Partial Fulfillment of the Requirements for the Master's Degree

.....Dean of the Faculty of Medicine  
(Associate Professor Sophon Napathorn, M.D.)

THESIS COMMITTEE

.....Chairman  
(Assistant Professor Jaturon Tantivatana, M.D.)

.....Thesis Advisor  
(Associate Professor Anchali Krisanachinda, Ph.D.)

.....Thesis Co-advisor  
(Associate Professor Sukalaya Lerdlum, M.D.)

.....External Examiner  
(Professor Franco Milano, Ph.D.)

ณัฐพงศ์ ด้านธนวัฒน์ : ผลกระทบ Echo Time, Echo train length และ Flip angle เพื่อลด chemical shift artifact ใน T2 weighted โดยเทคนิค turbo spin echo pulse sequence (Effect of Echo Time, Echo Train Length and Flip Angle of T2 Weighted Turbo Spin Echo in Reduction Chemical Shift Artifact) อ. ที่ปรึกษาวิทยานิพนธ์หลัก: รศ.ดร.อัญชติ กฤษณจินดา, อ.ที่ปรึกษาวิทยานิพนธ์ร่วม: รศ.พญ.สุกัลยา เลิศล้ำ, 43 หน้า.

เครื่องสร้างภาพด้วยเรโซแนนซ์แม่เหล็ก(MRI)มีความจำเป็นในหน่วยรังสีวินิจฉัย การตรวจกระดูกไขสันหลังและหมอนรองกระดูกเป็นที่นิยมกันอย่างแพร่หลาย เครื่องสร้างภาพด้วยเรโซแนนซ์แม่เหล็กสามารถใช้สร้างภาพกระดูกไขสันหลังได้ดีกว่าการตรวจด้วยเครื่องมือชนิดอื่น การเกิดสิ่งแปลกปลอมจากผลของพัลส์โมเลกุลที่ต่างกันอาจทำให้การวินิจฉัยผิดพลาด สิ่งแปลกปลอมชนิดนี้เกิดในแนวอครหัสโดยใช้ความถี่ เครื่องสนามแม่เหล็กกำหนดใช้ความถี่ในการระบุตำแหน่งของการสร้างภาพ สิ่งแปลกปลอมจากผลของพัลส์โมเลกุลที่ต่างกันจะเกิดบริเวณรอยต่อของน้ำและไขมัน จุดประสงค์ของการศึกษา คือ การปรับ Echo Time, Echo train length และ Flip angle อย่างเหมาะสมเพื่อลดการเกิดสิ่งแปลกปลอมจากผลของพัลส์โมเลกุลที่ต่างกัน โดยทดลองกับหุ่นจำลองทำด้วยอะคริลิกซึ่งภายในบรรจุน้ำและไขมัน และในการศึกษาจะทำการสร้างภาพโดยควบคุมตัวแปร ช่วงความถี่, ความละเอียดของภาพ, ขอบเขตของการสร้างภาพ และ แนวของการอครหัสความถี่ ใช้เทคนิค Turbo spin echo pulse sequence เพื่อลดความไม่สม่ำเสมอของสนามแม่เหล็กโดยใช้คลื่นวิทยุ 180 องศา ในการชดเชยความไม่สม่ำเสมอของสนามแม่เหล็ก การศึกษาจะสนใจใน T2 weighted โดยการปรับเปลี่ยน echo time, echo train length และ flip angle โดยใช้เครื่องสร้างภาพด้วยเรโซแนนซ์แม่เหล็ก 1.5 เทสลา ผลิตภัณฑ์ ซิเมน รุ่น Magnetom Essenza

การศึกษาวัดขนาดสิ่งแปลกปลอมจากผลของพัลส์โมเลกุลที่ต่างกัน โดยใช้โปรแกรม image J Flip angle แปรผันแบบผกผันกับขนาดสิ่งแปลกปลอมจากผลของพัลส์โมเลกุลที่ต่างกัน บริเวณตรงกลางของสิ่งแปลกปลอมจากผลของพัลส์โมเลกุลที่ต่างกันจะมีขนาดน้อยกว่าบริเวณขอบซ้ายและขวา และในการสร้างภาพ ภาพที่อยู่ตรงกลางของการสร้างภาพจะมีขนาดของสิ่งแปลกปลอมจากผลของพัลส์โมเลกุลที่ต่างกันน้อยกว่าภาพที่อยู่ตรงขอบของการสร้างภาพ Echo time แปรผันตรงกับขนาดสิ่งแปลกปลอมจากผลของพัลส์โมเลกุลที่ต่างกัน แต่ความสัมพันธ์ของ Echo train length กับขนาดสิ่งแปลกปลอมจากผลของพัลส์โมเลกุลที่ต่างกัน ไม่เป็นที่แน่ชัด

ภาควิชา .....รังสีวิทยา .....ลายมือชื่อนิสิต .....

สาขาวิชา .....สาขาเวชศาสตร์ .....ลายมือชื่อ อ.ที่ปรึกษาวิทยานิพนธ์หลัก .....

ปีการศึกษา .....2555 .....ลายมือชื่อ อ.ที่ปรึกษาวิทยานิพนธ์ร่วม .....

# # 5474118430 : Major MEDICAL IMAGING

KEYWORD : CHEMICAL SHIFT ARTIFACT/ T2 WEIGHTED/TURBO SPIN ECHO /

ECHO TIME

NUTTAPONG DANTHANAVAT: EFFECT OF ECHO TIME, ECHO TRAIN LENGTH AND FLIP ANGLE OF T2 WEIGHTED TURBO SPIN ECHO IN REDUCTION CHEMICAL SHIFT ARTIFACT. ADVISOR : ANCHALI KRISANACHINDA, Ph.D, CO – ADVISOR SUKALAYA LERDLUM,M.D, 43 pp.

Magnetic resonance imaging (MRI) is an essential part in diagnostic radiology. The effectiveness of magnetic resonance in evaluating the spine and intervertebral disks has become most favorite examination, as MRI can show anatomy of spine imaging better than other modality. Chemical shift artifact may cause pitfall of diagnostic. It occurs in the frequency encode direction. The MRI uses the frequency of the signal to indicate spatial position. Chemical shift artifact were occurred between fat and water interface. The objective of the study is to optimize echo time, echo train length and flip angle in T2 weighted Turbo spin echo for the chemical shift artifact reduction, in vitro study . Acrylic phantom was built and used by fill the water and vegetable oil in the phantom. Bandwidth, matrix size , field of view and frequency encoding direction were fixed in scanning.Turbo spin echo pulse sequence was used for compensation of magnetic field inhomogeneity due to rephrasing by 180 RF pulse. T2 weighted was used. Variable echo time, echo train length and flip angle were regarded for MRI 1.5 Tesla Siemens Model Magnetom Essenza.

Chemical shift artifact distances were measured by image J program. Flip angle are revert proportional to chemical shift artifact distances. Center position of artifact distance between fat and water interface is less than right and left position in the same slice (image). At different slice, center of slice selection shows artifact distance less than border of slice selection. Echo time are directly proportional to chemical shift artifact distances but echo train length are not clearly related to chemical shift artifact distances.

Department : ..... Radiology ..... Student's Signature .....

Field of Study : ... Medical Imaging ..... Advisor's Signature .....

Academic Year : ..... 2012 ..... Co-advisor's Signature .....

## ACKNOWLEDGEMENTS

I would like to express gratitude and deepest appreciation to Associate Professor Anchali Krisanachinda, Ph.D., Department of Radiology, Faculty of Medicine, Chulalongkorn University, my advisor, for her guidance, helpful suggestion, supervision, constructive comments and polishing of the thesis writing to improve the readability and English expression.

I would like to extremely greatly Associate Professor Sukalaya Lerdlum, M.D., Department of Radiology, Faculty of Medicine, Chulalongkorn University, for her advice and comments in the research

I would like to extremely thank to Associate Professor Sivalee Suriyapee, M.Sc., Department of Radiology, Faculty of Medicine, Chulalongkorn University for her invaluable advices, constructive comments.

I would like to extremely thank to Mr. Adun Kampangtip, M.Sc., for his suggestion, improvement and support.

I would like to extremely thank to Mr. Taweap Sanghangthum, Ph.D, Mr. Sornjarod Oonsiri, M.Sc., Ms. Puntiva Oonsiri M.Sc., the medical physic staffs at Division of Radiation Oncology, Department of Radiology, ,King Chulalongkorn Memorial Hospital, for their invaluable advices, constructive comments.

I would like to deeply thank to Professor Franco Milano, Ph.D. from University of Florence Italy, who is the external examiner of this thesis defense for his helpful recommendations, constructive comments and teaching of knowledge in Medical Imaging.

I would like to deeply thank to Paolo Memorial Hospital for support my experiment by using MRI

I would like to thank Mrs. Weeranuch Kitsukjit for her provide suggestion for the improvement.

Finally, I am extremely grateful for all teachers, lecturers and staffs at Master of Science Program in Medical Imaging, Faculty of Medicine, Chulalongkorn University for their help, and unlimited teaching of knowledge during the course in Medical Imaging. My grateful is forwarded to the Graduate Studies for supply the knowledge as tutor, especially, Dr. Kitiwat Khamwan for his contribution in part data analysis and every suggestions.

## CONTENTS

	<b>Pages</b>
ABSTRACT (THAI).....	iv
ABSTRACT (ENGLISH).....	v
ACKNOWLEDGEMENTS.....	vi
CONTENTS.....	vii
LIST OF TABLES.....	ix
LIST OF FIGURES.....	x
LIST OF ABBREVIATIONS.....	xii
<b>CHAPTER I INTRODUCTION</b>	
1.1 Background and rationale.....	1
1.2 Research objective.....	2
<b>CHAPTER II REVIEW OF RELATED LITERATURE</b>	
2.1 Theory.....	3
2.1.1 The introduction of MRI.....	3
2.1.2 Chemical shift artifact .....	3
2.1.3 Bandwidth .....	5
2.1.4 Magnetic field strength.....	6
2.1.5 Spin echo imaging method.....	7
2.1.6 Flip angle .....	14
2.2 Review of Related Literature.....	14
<b>CHAPTER III RESEARCH METHODOLOGY</b>	
3.1 Research design.....	17
3.2 Research design model.....	17
3.3 Conceptual framework.....	17
3.4 Research questions.....	18
3.5 Materials.....	18
3.5.1 MRI 1.5 Tesla, Siemens, Magnetom Essenza.....	18
3.5.2 6-element Head matrix coil .....	18
3.5.3 Acrylic Phantom .....	19
3.5.4 ACR MRI phantom.....	19
3.5.5 Image J program .....	20

	<b>Pages</b>
3.6 Methods.....	20
3.6.1 QC for MRI scanner.....	20
3.6.2 Design and construct an acrylic phantom.....	20
3.6.3 MRI scanning techniques .....	21
3.7 Data analysis.....	22
3.7.1 Image evaluation.....	22
3.7.2 Artifact distance measurement .....	22
3.8 Sample size determination.....	22
3.9 Statistical analysis.....	22
3.10 Outcome measurement.....	22
3.11 Expected benefits.....	22
3.12 Ethical consideration.....	22
<b>CHAPTER IV RESULTS</b>	
4.1 Quality control of MRI scanner.....	23
4.2 Chemical shift artifact measurement data .....	23
4.2.1 Evaluation of the artifact distance .....	23
<b>CHAPTER V DISCUSSION AND CONCLUSION</b>	
5.1 Discussion.....	27
5.1.1 Assessment of chemical shift artifact in echo time (TE)	27
5.1.2 Assessment of chemical shift artifact in flip angle	27
5.1.3 Assessment of chemical shift artifact in echo train length	28
5.1.4 Assessment of chemical shift artifact in different slice number and position of artifact in the image .....	29
5.2 Study Limitations.....	29
5.3 Conclusions.....	29
<b>REFERENCES</b> .....	30
<b>APPENDICES</b> .....	31
Appendix A.....	32
Appendix B.....	34
<b>VITAE</b> .....	43



## LIST OF TABLES

<b>Table</b>		<b>Pages</b>
4.1	Report of MRI systems 1.5 T performance test.....	23
4.2	The mean of chemical shift artifact distance when compared echo train length 10, 15, 20, 25, 30 per slice in the same flip angle 120 degree and echo time 82 msec.....	23
4.3	The mean of chemical shift artifact distance when compared echo time 82, 99, 115 in the same flip angle 120 degree and echo train length 10 per slice.....	24
4.4	The mean of chemical shift artifact distance when compared flip angle 120, 150,180 degree in the same echo time 82 msec and echo train length 10 per slice.....	25

## LIST OF FIGURES

<b>Figure</b>		<b>Pages</b>
2.1	Chemical shift artifact occurs in the frequency encode direction	4
2.2	Chemical shift misregistration artifact manifests as bright or dark outlines predominantly at fat / water interfaces.....	4
2.3	Chemical-Shift Artifact.....	6
2.4	The spin echo process use of 180° pulse to rephrase the protons and to produce an echo event.....	8
2.5	The 180° pulse set up the proton so that they rephrase.....	9
2.6	The RF pulses and time intervals in a spin echo imaging cycle.....	9
2.7	Turbo spin echo pulse sequence multiple echoes are created following a single excitation pulse. Each echo is a spin echo refocused by a 180° refocusing pulse.....	11
2.8	For a given echo train, the effective TE with turbo spin echo imaging can be varied by changing the order of the phase encoding steps; the effective TE is defined by the timing of zero phase encoding (A) effective TE is defined by the middle echo in echo train. (B) effective TE is defined by the first echo	12
2.9	Acquisition efficiency with the multislice turbo spin echo technique	13
2.10	Effect of echo spacing on acquisition efficiency. With shorter echo spacing the echo train length can be increased without reducing the number of image slice obtained at a given TR.	14
3.1	MRI 1.5 Tesla, (Siemens Health care: Magnetom Essenza).....	18
3.2	6-element Head matrix coil.....	18
3.3	Acrylic Phantom.....	19
3.4	ACR MRI phantom.....	19
3.5	Fill the phantom with water, bottom, and vegetable oil, top, each of 7.5 cm height.....	20
4.1	The mean of chemical shift artifact distance when compared echo time 82, 99, 115 in the same flip angle 120 degree and echo train length 10 per slice.....	24
4.2	The mean of chemical shift artifact distance when compared flip angle 120, 150, 180 degree in the same echo time 82 msec and echo train length 10 per slice.....	25
4.3	The mean of chemical shift artifact distance when compared slice number 1, 6 and 11 in the same echo time, echo train length and flip angle.....	26

<b>Figure</b>		<b>Pages</b>
5.1	Chemical shift artifact was compared between echo time 82 msec (a) and 115 (b) msec when fixed other scanning parameters.....	27
5.2	Chemical shift artifact was compared between flip angle 120 degree (a) and 180 degree (b) when fixed other scanning parameters.....	28
5.3	Chemical shift artifact was compared in echo train length 10, 15, 20, 25 and 30 per slice, flip angle 120 when echo time 82 msec (a) and echo time 115 msec (b).....	28

## LIST OF ABBREVIATION

<b>ABBREVIATION</b>	<b>TERMS</b>
AAPM	American Association of Physicists in Medicine
ACR	American College of Radiology
$B_0$	Magnetic field strength
$B_1$	Radio frequency field strength
ETL	Echo train length
FID	Free induction decay
FOV	Field of view
FSE	Fast spin echo
IR	Inversion recovery
MRI	Magnetic resonance imaging
MRS	Magnetic resonance spectroscopy
NSA	Number of average
RF	Radiofrequency
SE	Spin echo
TE	Echo time
TR	Repetition time
TSE	Turbo spin echo

# CHAPTER I

## INTRODUCTION

### 1.1 Background and Rationale

The magnetic resonance imaging (MRI) has become the favorite modality. Currently there is more research to improve potential of this modality. MRI is not significantly hazard from ionizing radiation. MRI is more versatile than the X-rays and is used to examine a large variety of medical conditions and it possible to visualize and analyze a variety of tissue characteristic, blood flow, several physiologic and metabolic functions. Much of this power comes from the ability to adjust the imaging process to be especially sensitive to each of the characteristics being evaluated. A lot of parameters concerns in image quality than other modality which can show different tissue contrast image in each pulse sequence enhance something which radiologist wishes to detect. The physicians who requested and the radiologists who interpret the MRI examination wish to obtain the quality image to get the accurate diagnosis.

MRI is a fairly new technique that has been used since the beginning of the 1980. The effectiveness of magnetic resonance in evaluating the spine and intervertebral disks has become most favorite examination. As MRI can show anatomy of spine imaging better than other modality, the neuro physician tends to request spine MRI imaging for diagnosis such as spinal stenosis, deformities of the spine, spondylolysis (degenerative disease), hernia of intervertebral disc, infection of spine, spinal cord compression etc. . MRI pulse sequence creates the vary tissue contrast characteristic with more parameters adjusted to improve image quality. The spine is probably the most difficult part of the skeletal system to be evaluated by the radiograph because its complexity. The appropriate use of this technology is still in progress. Image artifact is occurred in MRI image by several reasons and different types of artifact.

An image artifact is a feature appears in an image which is not present in the original object. It is sometimes the result of improper operation of the imager, a consequence of natural processes or properties of the human body. There are numerous kinds of artifacts that can occur in MRI such as aliasing, truncation, crosstalk, motion, susceptibility and etc. It affects the quality of the MR images and make confused with pathology. Chemical shift artifact is one type of artifact cause erroneous diagnostic. Both fat and water are more consisted in human body composition of each part in human organ. Fat and water interface can bring chemical shift artifact. The chemical shift artifact is caused by the difference in Larmor frequency of fat and water. It depends on magnetic field strength and bandwidth. This artifact is almost occurred in all part of human organ image such as spine image, to show at the vertebral body end plate (black line is prominent at the interface between the disk and the upper surface of the vertebra) and may cause pitfall of diagnostic. It occurs in the frequency encode direction. The MRI uses the frequency of the signal to indicate spatial position. Since water consisted in this part organs resonate different than fat. It makes mistake of the frequency difference as a spatial position and increase when magnetic field strength increases from 1.5 T to 3 T. This artifact can be over estimate or under estimate in the lesion of spine which the radiologist may not overlook this artifact. In order to optimize MRI procedure for a specific clinical

examination, the operator must have good knowledge of the MRI and how those characteristics can be controlled.

### **1.2 Research Objective**

To optimize the echo time, echo train length and flip angle in T2 weighted Turbo spin echo for the chemical shift artifact reduction

## **CHAPTER 2**

### **REVIEW OF RELATED LITERATUES**

#### **2.1 Theory**

##### **2.1.1 The introduction of MRI [1]**

The Magnetic Resonance Imaging (MRI) was discovered in the 1950s and for many years its major application was in the field of spectroscopy; discerning chemical species from the inherent shift in resonant frequency exhibited by nuclei which depends on their chemical environment. Until the 1970s when Lauterbur introduced the concept of magnetic field gradients, an image based on magnetic resonance could be produced. By the 1980s whole body magnets were being produced in England permitting the first in vivo images of human anatomy. Today the technique, known as MR imaging, is widespread and an estimated 20 million scans are performed worldwide each year. It provides images with excellent soft-tissue contrast which can be acquired in any imaging plane, and unlike CT it does not involve the use of ionizing radiation. It is the imaging modality of choice in brain spinal cord and musculoskeletal for routinely use in many other clinical settings.

Magnetic resonance imaging (MRI) has provided high temporal, spatial, and contrast resolution methods to assess structure. However, the need to assess beyond the purely anatomic aspects, such as biochemistry and tissue physiology, required the development of functional techniques such as functional magnetic resonance imaging (fMRI), perfusion weighted imaging (PWI), and diffusion weighted imaging (DWI), and magnetic resonance spectroscopy (MRS).

In selecting pulse sequences and measurement parameters for a specific application, MRI allows the user tremendous flexibility to produce variation in contrast between normal and diseased tissue. This flexibility is available when imaging both stationary tissues as well as flowing blood. For example: technique bright-blood and dark-blood. A typical patient examination acquires sets of images with multiple types of contrast (proton density, T1, T2) and multiple slice orientations (transverse, sagittal, coronal, oblique), providing the clinician with more complete information on the nature of the tissue under observation and increasing the likelihood of lesion detection. It is important that the MR examinations be tailored to the organ or organs under investigation, the type of disease process, and the individual patient. The MR physician may choose to provide detailed measurement parameters for each examination, or have a predetermined regimen of scans performed by a technologist. Establishing fixed measurement protocols to ensure reliable, reproducible imaging examinations are performed.

##### **2.1.2 Chemical shift artifact [2]**

Chemical shift artifact is a common finding on some MRI sequences and used in MRS. Chemical shift is due to the differences between resonance frequencies between fat and water. It occurs in the frequency encode direction where a shift in the detected anatomy occurs because fat resonates at a slightly lower frequency than water. Essentially it is due to the effect of the electron cloud to greater or lesser degree shielding the nucleus from the external static magnetic field ( $B_0$ ). The Larmor frequency determines the frequency at which a particular nucleus resonates is established at the nucleus, and therefore different tissues will have slightly different Larmor frequencies depending on their chemical composition.

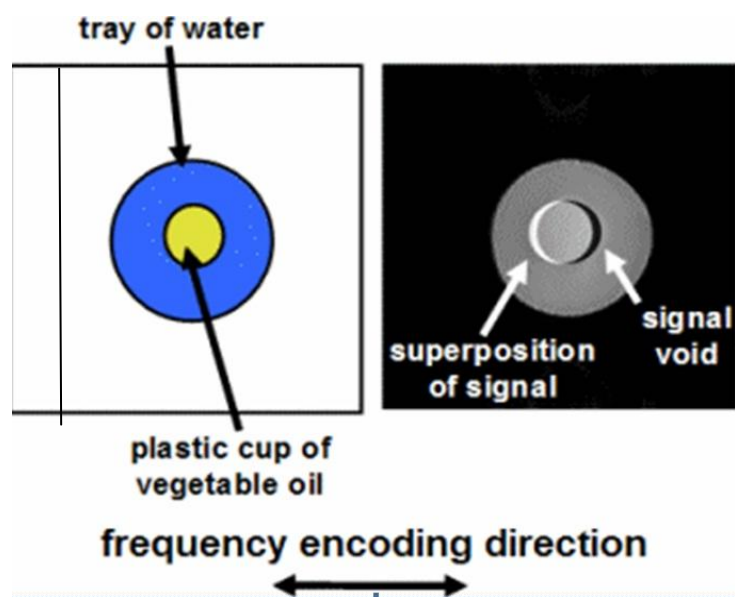


**Figure 2.1** Chemical shift artifact occurs in the frequency encode direction where a shift in the detected anatomy occurs because fat resonates at a slightly lower frequency than water.

During frequency encoding, fat protons precess slower than water protons in the same slice because of their magnetic shielding. Through the difference in resonance frequency between water and fat, protons at the same location are misregistered (dislocated) by the Fourier transformation, when converting MRI signals from frequency to spatial domain. This chemical shift misregistration cause accentuation of any fat-water interfaces along the frequency axis and may be mistaken for pathology. Where fat and water are in the same location, this artifact can be seen as a bright or dark band at the edge of the anatomy.

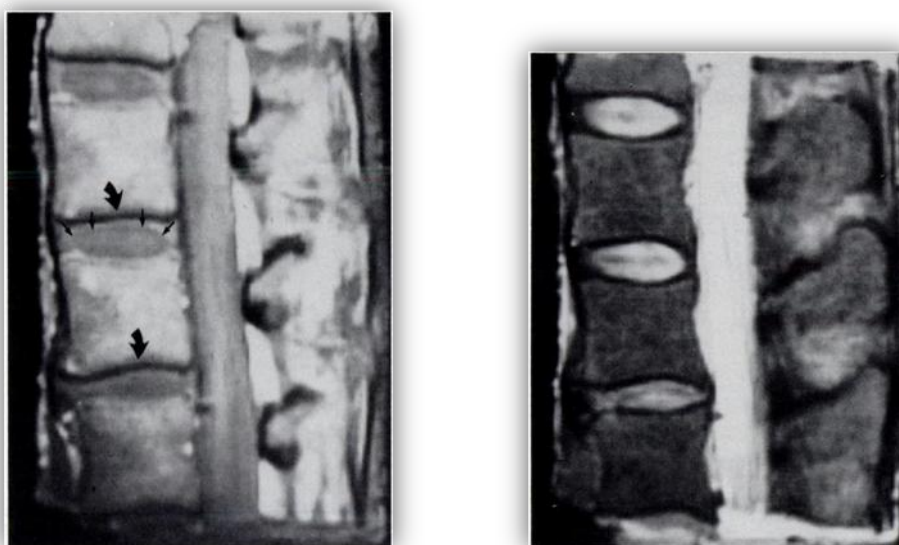


**Figure 2.2** Chemical shift misregistration artifact manifests as bright or dark outlines predominantly at fat / water interfaces



## Bandwidth

Chemical shift depends upon the band width. Narrow bandwidth higher cause the chemical shift increased. (BW) Bandwidth is a measure of frequency range, the range between the highest and lowest frequency allowed in the signal. For analog signals, which can be mathematically viewed as a function of time, bandwidth is the width, measured in Hertz of a frequency range in which the signal's Fourier transform is nonzero.

The receiver (or acquisition) bandwidth (rBW) is the range of frequencies accepted by the receiver to sample the MR signal. The receiver bandwidth is changeable (see also acronyms for 'bandwidth' from different manufacturers) and has a direct relationship to the signal to noise ratio (SNR) ( $SNR = 1/\text{square root (rBW)}$ ). The bandwidth depends on the readout (or frequency encoding) gradient strength and the data sampling rate (or dwell time). Bandwidth is defined by

$$BW = \text{Sampling Rate}/\text{Number of Samples.}$$

A smaller bandwidth improves SNR, but can cause spatial distortions, also increases the chemical shift. A larger bandwidth reduces SNR (more noise from the outskirts of the spectrum), but allows faster imaging.

The transmit bandwidth refers to the RF excitation pulse required for slice selection in a pulse sequence. The slice thickness is proportional to the bandwidth of the RF pulse (and inversely proportional to the applied gradient strength). Lowering the pulse bandwidth can reduce the slice thickness.

A higher bandwidth is used for the reduction of chemical shift artifacts (lower bandwidth - more chemical shift - longer dwell time - but better signal to noise ratio). Narrow receive bandwidths accentuate this water fat shift by assigning a smaller number of frequencies across the MRI image. This effect is much more significant on higher field strengths. At 1.5 T, fat and water precess 220 Hz apart, which results in a higher shift than in Low Field MRI. Lower bandwidth (measured in Hz) = higher water fat shift (measured in pixel shift).

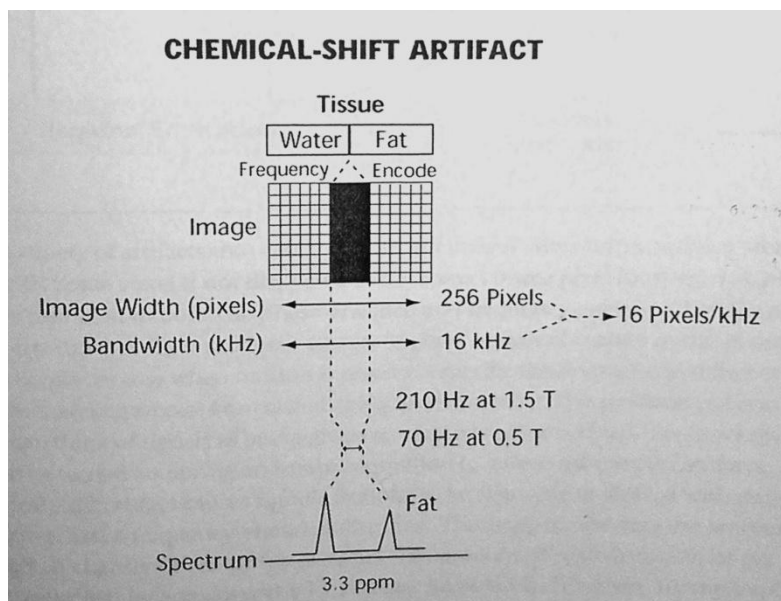


**Figure 2.3** Chemical-Shift artifact

Assume a bandwidth of 16 kHz. If the image matrix is 256 pixels in the frequency encode direction, this give 16 pixels per kHz of frequency (256 pixels/16kHz). If we now multiply this by the chemical shift of 0.210 kHz (210 Hz), we see that the chemical shift will be 3.4 pixels.

### Magnetic field strength

Chemical shift increases with magnetic field strength. Protons in fat and water molecules are separated by a chemical shift of about 3.5 ppm. The actual shift in Hertz (Hz) depends on the magnetic field strength of the magnet being used. Higher field strength increases the misregistration, while in contrast a higher gradient strength has a positive effect. The amount of chemical shift is often expressed in arbitrary units known as parts per million (ppm) of the main magnetic field strength. It's value is always independent of the main field strength and equals 3.5 ppm for fat and water, however the precessional frequency is proportional to the main magnetic field strength  $B_0$ , for example, at 1.5 T the difference in precessional frequency is 224 Hz. That is, fat precesses 224 Hz less than water. At 1.0 T this difference is 147Hz at lower field strengths (0.5 T or less), it is usually insignificant

In MRS the shift in Larmor frequency allows separation of different chemical peaks. The actual amount of chemical shift as an absolute value is difficult to measure, so instead it is represented relative to a reference, and expressed in parts per million (ppm).

In MRI, both spin echo sequences (SE) and gradient echo sequences (GE) may demonstrate chemical shift artifact, but it will appear differently depending on the sequence.

### **Spin echo imaging method [3]**

Spin echo is the name of the process that uses an RF pulse to produce the echo event. It is also the name for one of the specific imaging methods; all of which use the spin echo process.

#### **The spin echo process**

The decay of transverse magnetization (i.e., relaxation) occurs because of dephasing among individual nuclei. Let us recall that two basic conditions are required for transverse magnetization: (1) the magnetic moment of the nuclei must be oriented in the transverse direction, or plane, and (2) a majority of the moment must be in the same direction within the transverse plane. When a nucleus has a transverse orientation, it is actually precessing or rotating around an axis that is parallel to the magnetic field.

After the application of a 90° excitation pulse, the nuclei have a transverse orientation and are precessing together, or in phase, around the magnetic field axis. This is the normal precession discussed earlier but flipped into the transverse plane. However, within an individual voxel some nuclei precess or spin faster than others. After a short period of time, the nuclei are not spinning in phase. As the directions of the nuclei begin to spread, the magnetization of the tissue decreases. A short time later, the nuclei are randomly oriented in the transverse plane; there is no transverse magnetization.

The two factors that contribute to the dephasing of the nuclei and the resulting transverse relaxation will now be reviewed again here. One is an exchange among the spinning nuclei (spin-spin interaction), which results in relatively slow dephasing and loss of magnetization. The rate at which this occurs is determined by characteristics of the tissue. It is the dephasing activity that is characterized by the T2 values and the source of contrast that we want to capture in T2 images. A second factor, which produces relatively rapid dephasing of the nuclei and loss of the transverse magnetization, is the inhomogeneity of the magnetic field. Even within a small volume of tissue, the field inhomogeneities are sufficient to produce the rapid dephasing. This effect, which is generally unrelated to the T2 characteristic of the tissue, tends to mask the true relaxation characteristic of the tissue. In other words, the actual transverse magnetization relaxes much faster than the tissue characteristic would indicate. We remember that this real relaxation time is designated as T2\*. The value of the T2\* is always much less than the tissue T2 value. As a result, the transverse magnetization disappears before T2 contrast can be formed.

We are about to discover that spin echo is a process for recovering the loss of transverse magnetization and making it possible to produce an image of the tissue characteristic including T2.

An RF signal is produced whenever there is transverse magnetization. Immediately after an excitation pulse, a so-called free induction decay (FID) signal is produced. The intensity of the signal is proportional to the level of transverse magnetization. Both decay rather rapidly because of the magnetic field inhomogeneities just described. The FID signal is not used in the spin echo methods. It is used in the gradient echo methods.

The spin echo process is used to compensate for the dephasing and rapid relaxation caused by the field inhomogeneities and to restore the magnetization to the level that depends only on the tissue T2 characteristic. The sequence of events in the spin echo process is illustrated in figure 2.4.

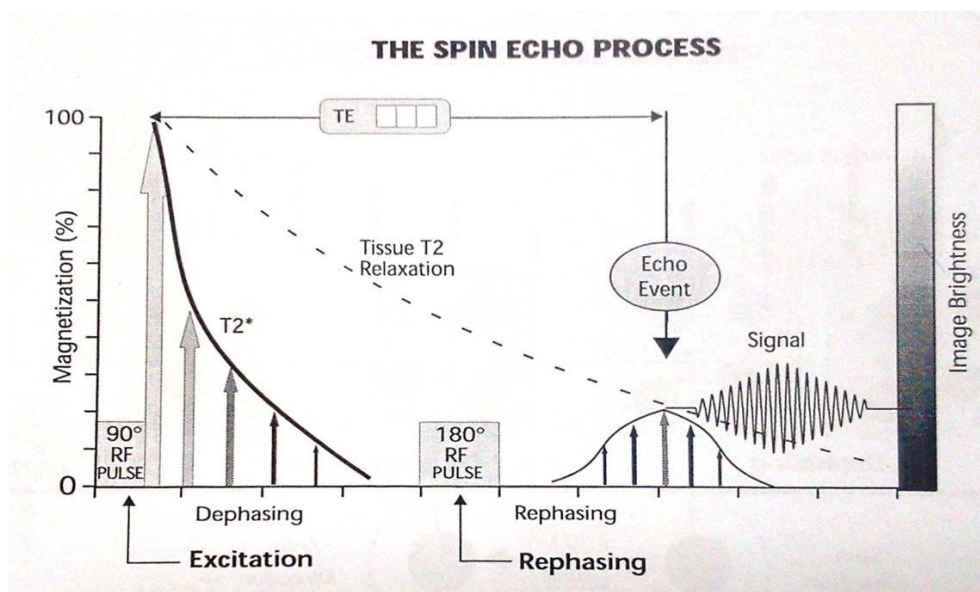


**Figure 2.4** the spin echo process showing the use of a  $180^\circ$  pulse to rephrase the protons and to produce an echo event.

Transverse magnetization is produced with a  $90^\circ$  RF excitation pulse that flips the longitudinal magnetization into the transverse plane. Immediately following the RF pulse, each voxel is magnetized in the transverse direction. However, because of the local magnetic field inhomogeneities within each voxel, the protons precess at different rates and quickly slip out of phase. This produces the rapid decay characterized by  $T2^*$  and the associated FID signal. At this time the protons are still rotating in the transverse plane, but they are out of phase.

If a  $180^\circ$  pulse is applied to the tissue containing these protons, it flips the protons around an axis in the transverse plane; this reverses their direction of rotation as illustrated in figure 1.5. This causes the fast protons to be located behind the slower ones. As the faster protons begin to catch up the slower ones, they regain a common alignment, or come back in to phase. This in turn, causes the transverse magnetization to reappear and form the echo event. However, the magnetization does not grow to the initial value because the relaxation (dephasing) produced by the tissue is not reversible. The rephrasing of the protons causes the magnetization to build up to the level determined by the  $T2$  characteristics of the tissue. As soon as the magnetization reaches this maximum, the protons begin to move out of phase again, and the transverse magnetization dissipates. Another  $180^\circ$  pulse can be used to produce another rephrasing. In fact, this is what is done in multi echo imaging.

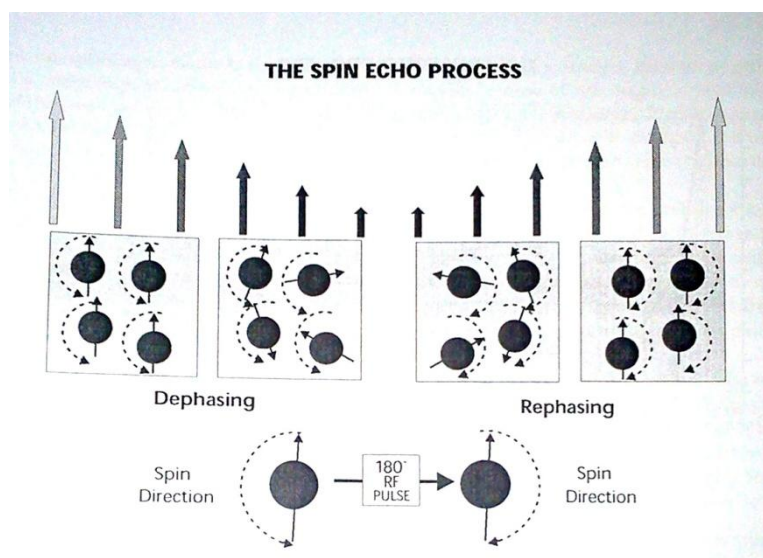


**Figure 2.5** The  $180^\circ$  pulse set the proton so that they rephase.

### RF pulse sequence

The difference imaging methods are produced by the type (Flip angle) and time intervals between the applied RF pulses.

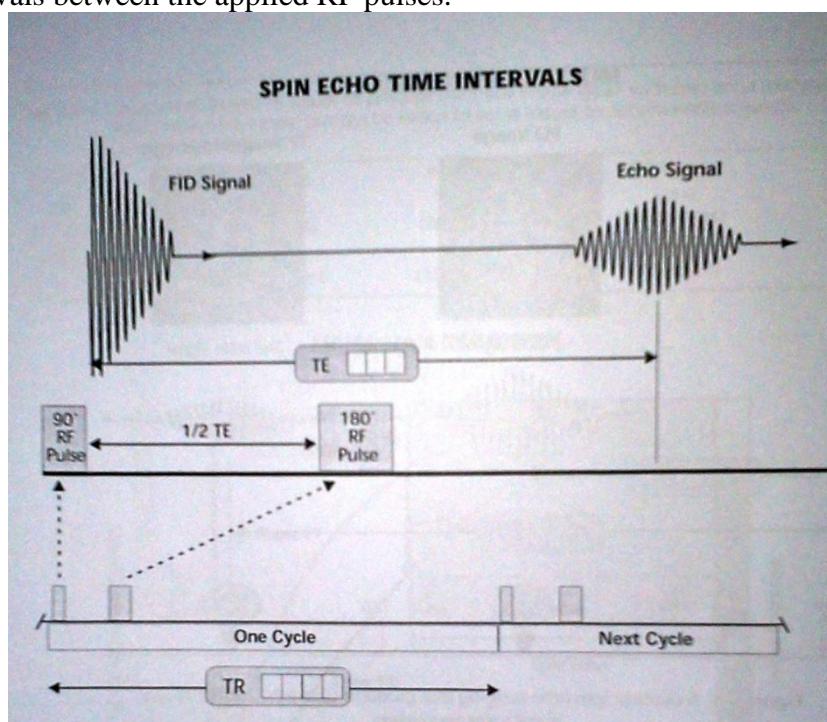


**Figure 2.6** The RF pulses and time intervals in a spin echo imaging cycle.

Each cycle begins with a  $90^\circ$  excitation pulse that produces the initial transverse magnetization and a later  $180^\circ$  pulse that rephases the proton to produce the echo event. The time between the initial excitation and the echo signal is TE. This is controlled by adjusting the time interval between the  $90^\circ$  and the  $180^\circ$  pulse, which is  $1/2$  TE.

### **The spin echo method**

This method can be used to produce images of the three basic tissue characteristic: PD, T1 and T2. The sensitivity to a specific characteristic is determined by the value selected for the two time intervals or imaging factors, TR and TE.

The process of creating image has three types of the contrast (PD, T1, T2). The type of image that was produced depended on the value selected for the two protocol factors, TR and TE. We will now review that process with a few more details specifically as it applies to the spin echo method.

#### **Proton density (PD) contrast**

PD contrast develops as the longitudinal magnetization approaches its maximum, which is determined by the PD of each specific tissue. Therefore, relatively long TR values are required to produce a PD weighted image. Short TE values are generally used to reduce T2 contrast contamination and to maintain relatively high signal intensity.

#### **T1 contrast**

To produce image contrast base on T1 difference between tissues, two factors must be considered. Since T1 contrast develops during the early growth phase of longitudinal magnetization, relatively short TR values must be used to capture the contrast. The second factor is to preserve the T1 contrast during the time of transverse relaxation. The basic problem is that if T2 contrast is allowed to develop, it generally counteracts T1 contrast. This is because tissues with short values usually have short T2 values. The problem arises because tissue with short T1 is generally bright, whereas tissue with short T2 has reduced brightness when T2 contrast is present. T2 contrast develops during the TE time interval. Therefore, a T1 weighted image is produce by using short T1 values and short TE values.

#### **T2 contrast**

The first step in producing an image with significant T2 contrast is to select a relatively long TR value. This minimizes T1 contrast contamination and transverse relaxation process begins at a relatively high level of magnetization. Long TE values are then use to allow T2 contrast time to develop. The spin echo method is the only method that produces true T2 contrast. That is because it is able to rephrase the protons and remove the T2\* effect.

### **Multiecho conjugate Technique**

Multiecho techniques can be used to decrease the acquisition time in single images and generate images with difference tissue contrast, as described above. With such techniques, difference phase encoding values are applied for each of the multiple echoes, so each echo fill a difference line of k- space in the same image. For such methods, some new terminology must be introduced. Each set of echoes that follows an excitation pulse is referred to as an echo train. The period during which these echoes are required is the echo train duration, and the number of echoes in the echo train is the echo train length (ETL). In Turbo spin echo involves acquiring multiple spin echoes following each pulse.

### **Fast spin echo or Turbo spin echo**

Fast (Turbo) spin echo images contain several excitation pulses, each of which is followed by a train of refocusing pulses that, in turn, generate a train of spin echoes. Each of these echoes is usually free degradation due to magnetic field and chemical shift heterogeneity. These images can have high spatial resolution and high SNR.

Although fast spin echo images are subject to blurring and edge artifact, these problem can be minimized by use of a high acquisition matrix and judicious choice of echo train length and effective TE.

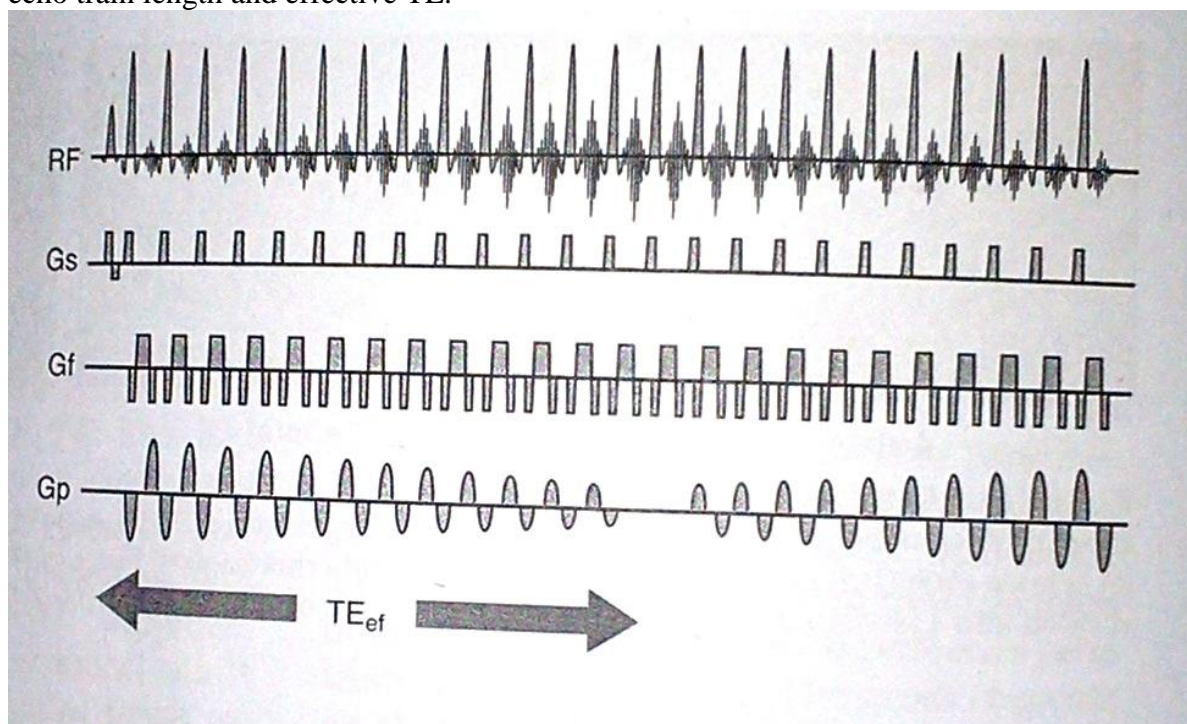


**Figure 2.7** Turbo spin echo pulse sequence multiple echoes are created following a single excitation pulse. Each echo is a spin echo refocused by a  $180^\circ$  refocusing pulse. The phase encoding gradient pulse that precedes each echo has a difference value, and each echo is followed by a rewinding gradient that restores phase.

In turbo spin echo techniques, most of the time is spent applying refocusing pulses and sampling echoes. The major gain in efficiency, compared with single echo spin echo techniques, is that during a given TE multiple echoes are acquired. This increases efficiency by a factor equal to the number of echoes obtained by the time the effective TE is reached. For example, if six echoes can be obtained in 90 msec, a turbo spin echo technique with an echo train of 6 and a effective TE of 90 msec is six times as efficient as a single echo technique with a TE of 90 msec. when the echo train length increase beyond six, however, fewer image slice can be acquired if the TR remains constant. To obtain the same number of image slices using a longer echo train. It is necessary to increase the TR. Thus, efficiency is not substantially improved once the echo train becomes longer than the effective TE contributes to image blurring but does not reduce the acquisition time of a multislice stack of image.

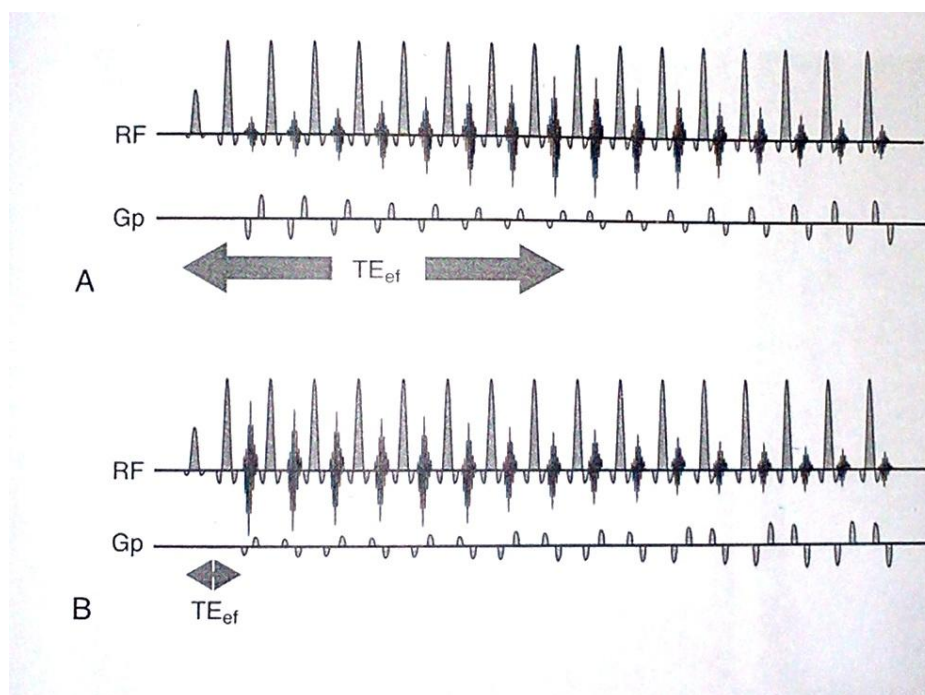


**Figure 2.8** For a given echo train, the effective TE with turbo spin echo imaging can be varied by changing the order of the phase encoding steps; the effective TE is defined by the timing of zero phase encoding. (A) effective TE is defined by the middle echo in echo train. (B) effective TE is defined by the first echo.

There are certain situations in which the echo train should increase beyond the effective TE, even though this could increase artifacts. Such situations include those in which the TR necessary to obtain the required number of image slices is shorter than the TR that would result in the desired tissue contrast or in which a short acquisition time is essential. In some instances, blurring in turbo spin echo images can, paradoxically, produce an appearance of edge enhancement. This is because blurring is greatest for tissue with a short T2 but minimal for those with a long T2. For example, simple fluid has crisp edges on long echo train images. Tissue with a short T2, however, has blurred edges. This causes some signal intensity to be mapped in adjacent pixels, increasing their apparent signal intensity. At the interface between fluid and tissues with a short T2, the short T2 tissue's signal intensity is smeared, overlapping the signal intensity of adjacent fluid. This produces artifactual edge enhancement because the periphery of the short T2 tissue has decreased signal intensity, whereas the margin of the long T2 tissue has increased signal intensity.



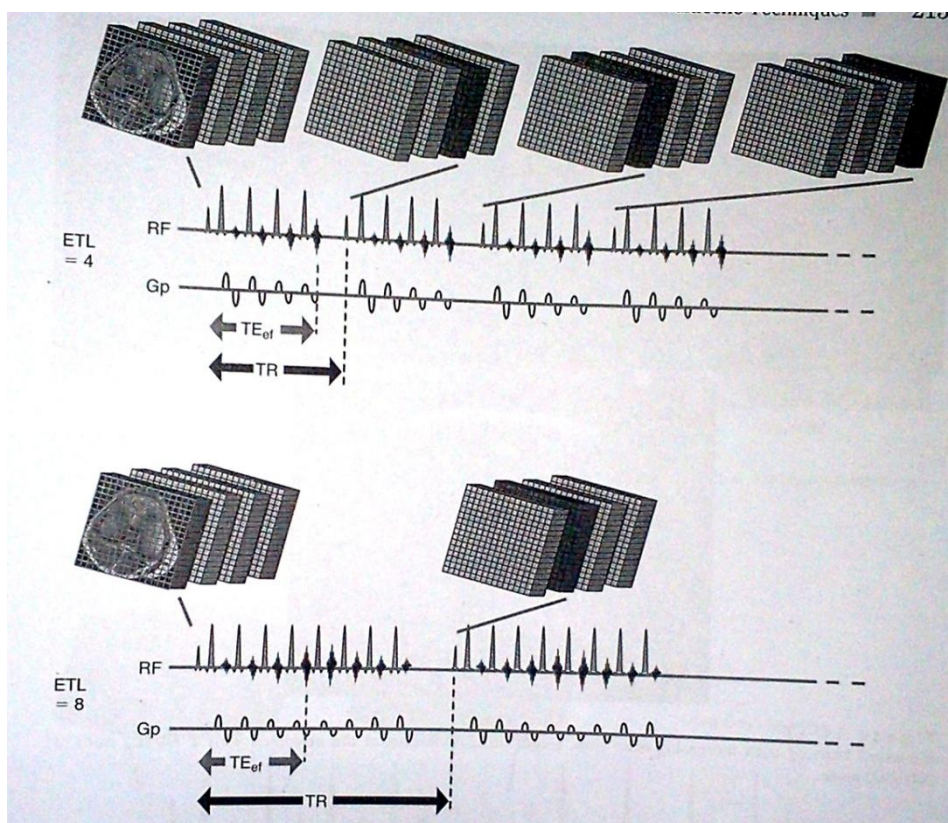


**Figure 2.9** Acquisition efficiency with the multislice turbo spin echo technique.

The multislice turbo spin echo technique is not necessarily improved by increasing the echo train length (ETL) beyond that needed for a given effective TE. In this example, with an ETL of 4 the effective TE is defined by the last echo. With an ETL of 8 the effective TE is unchanged, but only half as many image slice can be obtained during a given interval. To obtain the same number of image of slice with double the ETL, the TR must be approximately doubled.

A major determinant of efficiency with turbo spin echo techniques is echo spacing. If echoes are obtained rapidly, the echo train length can be long for a given echo train duration, decreasing the number of excitation that must be repeated. Tight echo spacing also reduces many artifacts associated with turbo spin echo. Therefore, minimizing echo spacing should be considered a priority when setting parameters for turbo spin echo pulse sequence.

Most turbo spin echo pulse sequence so as to minimize echo spacing; however, changes in bandwidth affect the duration of echo sampling and thus have a substantial effect on echo spacing. As the bandwidth increase, echo spacing can be decrease. For this reason, the sampling bandwidth should be as high as possible with turbo spin echo techniques unless it is limited by system hardware or the SNR. Recall that a wide bandwidth reduces the SNR.

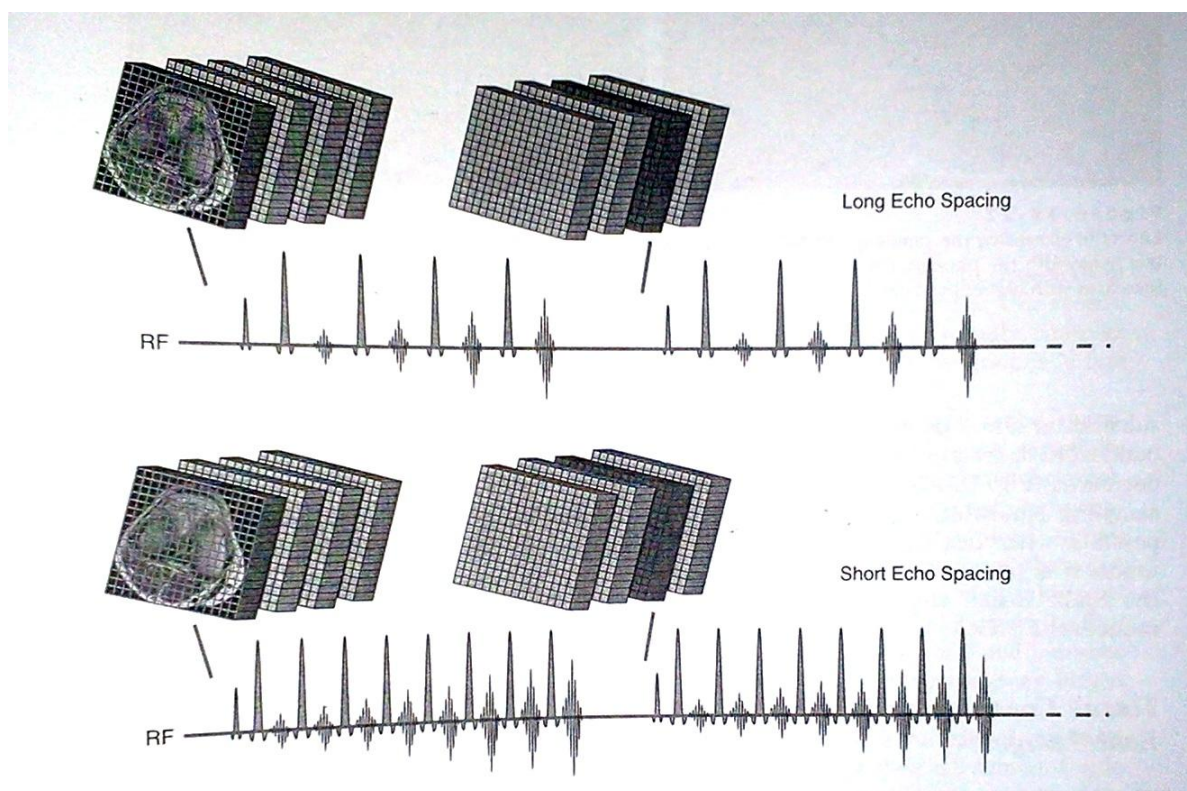


**Figure 2.10** Effect of echo spacing on acquisition efficiency. With shorter echo spacing the echo train length can be increased without reducing the number of image slice obtained at a given TR.

### Flip Angle

It is the angle to which the net magnetization is rotated or tipped relative to the main magnetic field direction via the application of a RF excitation pulse at the Larmor frequency. It is also referred to as the tip angle, nutation angle or angle of nutation. The radio frequency power (which is proportional to the square of the amplitude) of the pulse is proportional to a through which the spins are tilted under its influence. Flip angles between  $0^\circ$  and  $90^\circ$  are typically used in gradient echo sequences,  $90^\circ$  and a series of  $180^\circ$  pulses in spin echo sequences and an initial  $180^\circ$  pulse followed by a  $90^\circ$  and a  $180^\circ$  pulse in inversion recovery sequences.

### 2.2 Review of Related Literature

Robert C. Smith, MD Robert C. Lange, PhD., et al [4]. Chemical Shift Artifact: Dependence on Shape and Orientation of the Lipid-Water Interface. *Radiology* 18 (1991):225-229 Chemical shift artifact (CSA) can be seen at a planar lipid-water interface oriented within the plane of the phase-encoding and section-select directions (i.e. Perpendicular to the frequency-encoding direction). Phantoms and a clinical case were used to demonstrate that when a lipid-water interface is curvilinear (e.g., spherical) or planar but not oriented along the section-select direction, CSA may be absent or diminished. This effect can be seen at interfaces of normal structures (kidneys, bladder) as well as at interfaces with pathologic lesions such as lipid-containing dermoids. Not only is this effect dependent on section thickness, field of view, matrix size, and receiver bandwidth, but it is also strongly dependent on the orientation of the interface with respect to the section-select

direction. Knowledge of the factors that can alter CSA is important since it is used to distinguish lipid-containing from nonlipid-containing structures of similar signal intensities.

The results showed chemical shift artifact became absent was found to depend on section thickness, FOV, and orientation of the plane of section. With 5-mm-thick sections, CSA is readily seen through with 10-mm-thick sections, CSA is not visible.

Kalevi P. Soila, M.D, et al [5]. Chemical Shift Misregistration Effect in Magnetic Resonance Imaging Radiology 153(1984): 819-820. A low intensity artifact appearing at the junction of perirenal fat and renal parenchyma on MR images was recently described. A symmetrical high intensity artifact is also observable on the opposite side of the kidneys as well as at the junction of the right lobe of the liver and adjacent adipose tissue. Both artifacts can be explained as exhibitions of pixel misregistration due to the difference in chemical shifts of fatty and non-fatty organs. Identification of the chemical shift misregistration effect is important since the persistence of this artifact may cause erroneous diagnosis of calcification and/or fluid collections.

The result showed the chemical shift misregistration effect is a potentially serious problem in MR imaging. In the already difficult area of detection of small lesions, calcifications, and fluid collections it will create an additional source of uncertainty. It may also have a beneficial effect in delineating certain interfaces in critical areas such as cardiovascular imaging (heart vs. pericardial fat and arterial stenosis). The CSM effect will be more pronounced in high field instruments if gradient magnitudes are not increased linearly with the field strength to decrease the noise and limit the rate of magnetic field change (dB/dt) for multi-section and multi-echo imaging. This smaller relative gradient strength will cause the chemical shift separation to be larger in relation to the pixel frequency range.

Kampangtip A., Krisanachinda A., Singhara Na Ayudya S. (2012) Technical assessment of artifact production from endovascular coil at 3 Tesla MRI an in vitro study. 6<sup>th</sup> Annual Scientific Meeting, Phitsanulok, Thailand. Susceptibility artifacts and geometric distortions caused by magnetic field inhomogeneity-related signal loss is used to refer to an artifact in magnetic resonance images. It consists of a region of signal void with a surrounding area of an increased signal intensity that appears to be considerably larger than the actual size of the device causing the artifact. RF metal interaction effects were investigated systematically at  $B_0 = 3$  Tesla, analyzing correlated image artifacts for endovascular coils. The objective of the study is to compare the size of the artifact on the MR image to the actual size of endovascular coils using a 3 Tesla magnetic resonance imaging system, in vitro study. Endovascular coils were made from detachable platinum coils and aneurysm models were constructed by using catheters. A drop of gadolinium in normal saline solution was injected into each catheter. MRI 3 Tesla Philips Model Achieva. Pulse sequence selections were: Spin echo (conventional), fast spin echo, Inversion Recovery, Fast Gradient echo while additional parameters were Echo time and Turbo Factor.

The result showed spin echo for fast spin echo sequences are even better suited to reduce metal artifact. Furthermore, shorter turbo factor and shorter effective TE in the latter sequences are beneficial for the same reason as sequences having shorter TE. Sequences with a shorter TE are preferred because there is less time for dephasing and frequency shifting. Imaging at gradient echo series increases

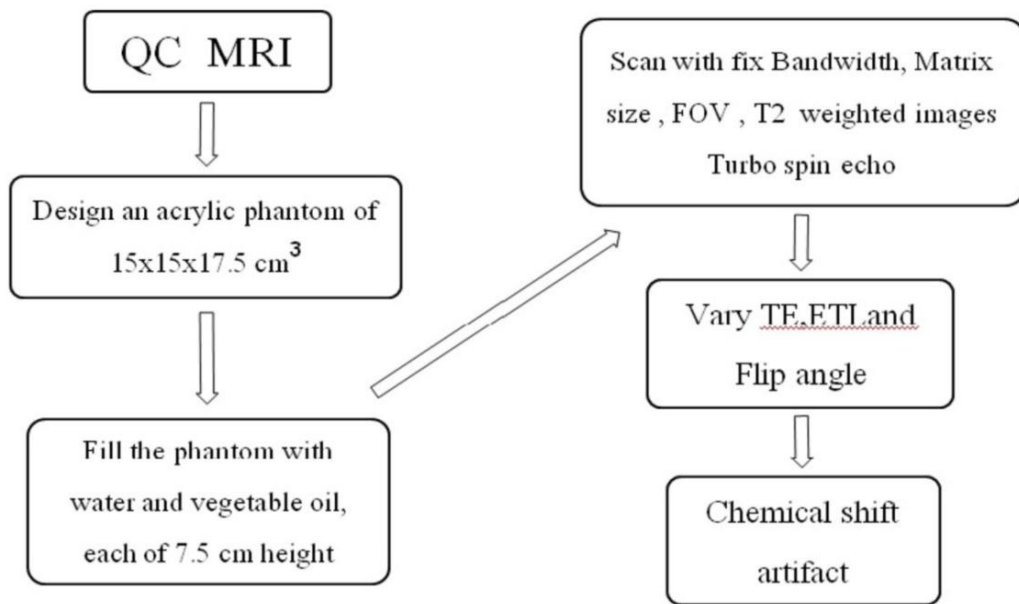
susceptibility artifacts. In this in vitro study, we have defined some of the major characteristics related to MRI imaging of coil packs. conclusions from this study are; 1) Pulse sequence Spin echo is best reduce susceptibility artifact; 2) Reducing the TE is the main factor in improving peri-aneurysmal visualization on MRI images; 3) The use of small field of view, high resolution matrix and thin slice can help reduce susceptibility artifacts. Artifacts are also produced in the frequency encoding

## CHAPTER III RESEARCH METHODOLOGY

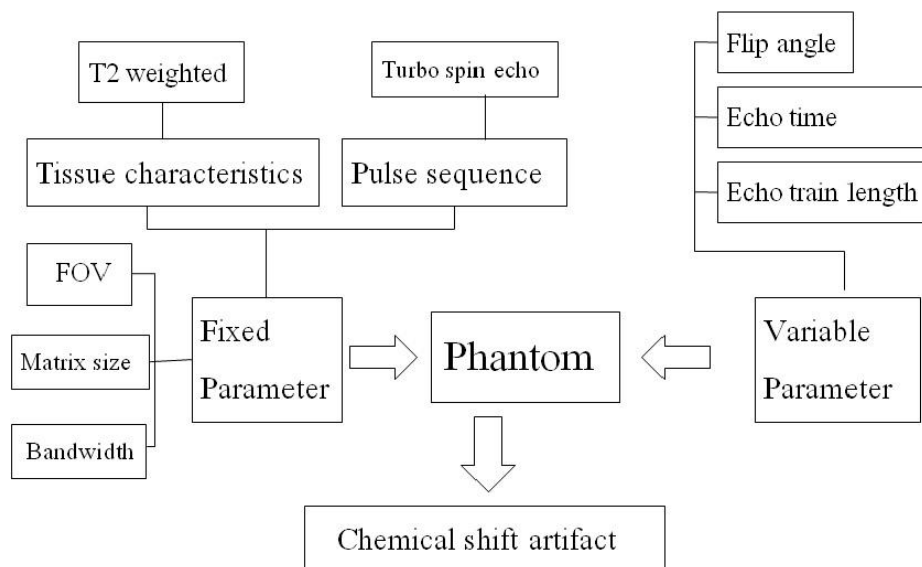
### 3.1 Research Design

This study is descriptive experimental research.

### 3.2 Research Design Model



### 3.3 Conceptual Framework



### 3.4 Research Questions

#### 3.4.1 Primary Question

What are the optimal echo time, echo train length and flip angle of T2 weighted Turbo spin echo pulse sequence for chemical shift artifact reduction?

### 3.5 Materials

#### 3.5.1 MRI 1.5 Tesla, Manufacturer Siemens Health care: Model Magnetom Essenza



**Figure 3.1** MRI 1.5 Tesla, (Siemens Health care: Magnetom Essenza) MRI 1.5 Tesla, at Department of Radiology, Paolo Memorial Hospital (Paholyothin) has been installed in 2009 (Syngo MR C13 application software for acquisition and processing).

#### 3.5.2 6-Element Head matrix coil



**Figure 3.2** 6-element Head matrix coil

6-element head matrix coil has been designed with 6 integrated preamplifiers. Upper coil part is removable and lower coil part is usable without upper part for highly claustrophobic patient. Lower coil part may stay on the patient table for most of the examinations with smoothly integrated into the patient table with Neck Matrix coil and Iso Center Matrix Coil.

### 3.5.3 Acrylic Phantom



**Figure 3.3** Acrylic phantoms

Simulation phantom sized 15cm width x15cm length x17.5 cm height was built using acrylic for filling water and vegetable oil each of 7.5 cm height. The water and vegetable oil height level were separated by black line

### 3.5.4 ACR MRI phantom

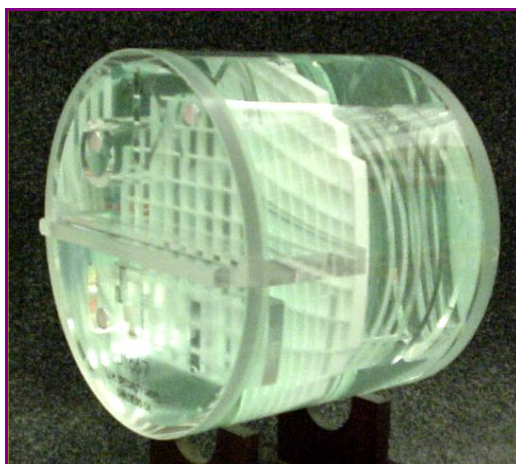


**Figure 3.4** ACR MRI phantoms

The ACR MRI accreditation phantom is constructed of acrylic plastic, glass, and silicone rubber. Ferromagnetic materials have been excluded. The phantom is a cylinder of 20.4 cm diameter by 16.5 cm length. Internal dimensions are 19.0 cm diameter by 15.0 cm length. The compact design allows placement in axial coronal, or sagittal orientation in almost all MRI head coils. Thus, tests can be conducted in all three major planes. There is a reference line down one side of the phantom.

### 3.5.5 Image J program

ImageJ is a public domain, Java-based image processing program developed at the National Institutes of Health. ImageJ was designed with an open architecture that provides extensibility via Java plugins and recordable macros. Custom acquisition, analysis and processing plugins can be developed using ImageJ's built-in editor and a Java compiler. ImageJ's plugin architecture and built in development environment has made it a popular platform for teaching image processing. ImageJ can display, edit, analyze, process, save, and print 8-bit color and grayscale, 16-bit integer and 32-bit floating point images. It can read many image formats including TIFF, PNG, GIF, JPEG, BMP, DICOM, FITS, as well as raw formats. ImageJ supports image stacks, a series of images that share a single window, and it is multithreaded, so time-consuming operations can be performed in parallel on multi-CPU hardware. ImageJ can be used to calculate area and pixel value statistics of user-defined selections and intensity threshold objects. It can measure distances and angles. It can create density histograms and line profile plots. It supports standard image processing functions such as logical and arithmetical operations between images, contrast manipulation, convolution, Fourier analysis, sharpening, smoothing, edge detection and median filtering. It does geometric transformations such as scaling, rotation and flips. The program supports any number of images simultaneously, limited only by available memory.

## 3.6 Methods

### 3.6.1 QC for MRI scanner

The quality control of MRI 1.5 Tesla was performed following the ACR manual (2004) and AAPM report No.100 (2010). The specific image parameters are: high contrast resolution, low contrast sensitivity, slice thickness, slice position, geometric distortion and image uniformity.

### 3.6.2 Design and construct an acrylic phantom

Acrylic phantom sized 15cm width x15cm length x17.5 cm height. Fill the phantom with water and vegetable oil, each of 7.5 cm height.

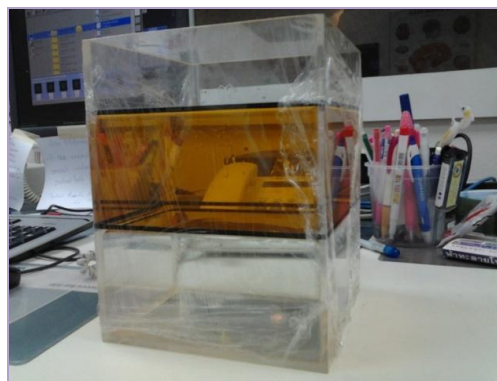


**Figure 3.5** Fill the phantom with water, bottom, and vegetable oil, top, each of 7.5 cm height



### **3.6.3 MRI scanning techniques**

The acrylic phantom was placed at the head matrix coil.

Scan the phantom with fixed parameters

FOV (20x20 cm<sup>2</sup>)

Matrix size (256x256)

Bandwidth (100 Hz/ Pixel)

Transverse plane, slice thickness 5 mm, gap 1mm, total of 11 slices

Scan with pulse sequence: Turbo spin echo: T2 weighted image by vary parameters

Echo train length: 10, 15, 20, 25, 30 per slice

Flip angle: 120, 150, 180 degree

Echo time: 82, 99, 115 msec

### **3.7 Data analysis**

#### **3.7.1 Image evaluation**

This research is an experimental study which the phantom simulated patient was used to the MR imaging examination at 1.5 Tesla

3.7.2 Artifact distance measurement using Image J program, at slice Number 1, 6 and 11

Bright or dark band (artifact) at the fat and water interface at slice center, right and left position of artifact images in same slice

### **3.8 Sample size determination**

This research will be performed in the phantom. The variation of subject (phantom) can be disregarded. Statistical variation for sample size is negligible. However, the phantom scan should be repeated more than once. Three times is considered (N=135)

### **3.9 Statistical analysis**

The artifact distance is analyzed as mean, standard deviation

### **3.10 Outcome measurement**

Size of bright or dark band (artifact) at the fat and water interface in each adjust Echo time, Echo train length and Flip angle.

### **3.11 Expected benefits**

Optimal Echo time, Echo train length and Flip angle of T2 weighted Turbo spin echo to reduce chemical shift artifact are obtained to improve protocols at the department.

### **3.12 Ethical consideration**

This research is an experimental study. Ethical consideration has been processed and approved in June 2012 by the ethic committee, Faculty of Medicine Chulalongkorn University.

## CHAPTER IV RESULTS

### 4.1 Quality control of MRI scanners

The quality control of MRI 3.0 Tesla, was performed by following the ACR Phantom manual (2008) [6], AAPM report No.100 (2010) [7]. The results of image uniformity, high contrast resolution, low contrast sensitivity, slice thickness, slice position/separation and geometric distortion are shown in Appendix B. The report of MRI system performance test is shown in Table 4.1

**Table 4.1** REPORT OF MRI SYSTEM 1.5 T PERFORMANCE TEST

<b>LOCATION</b>	Radiological department, Paolo memorial hospital
<b>DATE</b>	18 June, 2012
<b>MANUFACTURER</b>	SIEMENS Health care
<b>MODEL</b>	Magnetom Essenza 1.5 Tesla
<b>SOFTWARE VERSION</b>	Syngo MR C13
Geometric accuracy	pass
contrast spatial resolution	pass
Slice thickness accuracy	pass
Slice position accuracy	pass
Image intensity uniformity	pass
Percent-signal ghosting	pass
Low-contrast object detectability	pass

### 4.2 Chemical shift artifact Measurement Data

The distance measurements were detected in image J program.

#### 4.2.1 Evaluation of the artifact distance.

##### A. Variation of Echo train length

The result of the average from scanning three times in echo train length when compare in the same echo time and flip angle is shown in the table 4.2

**Table 4.2** The mean of chemical shift artifact distance when compared echo train length 10, 15, 20, 25, 30 per slice in the same flip angle 120 degree and echo time 82 msec

		Flip angle 120 TE 82					
mean			ETL 10	ETL 15	ETL 20	ETL 25	ETL 30
slice no.1	center		7.52±0.19	7.52±0.06	7.44±0.09	7.63±0.19	7.48±0.06
	right		8.15±0.1	8.45±0.33	7.67±0.09	8.11±0.16	7.71±0.16
	left		7.74±0.14	7.89±0.16	7.89±0.33	7.82±0.14	7.78±0.18
slice no.6	center		7.48±0.11	7.48±0.11	7.33±0.09	7.44±0.09	7.29±0.05
	right		8.11±0.09	7.63±0.21	7.52±0.26	7.89±0.09	7.85±0.21
	left		7.71±0.15	7.71±0.14	7.63±0.14	7.67±0.18	7.56±0.09
sliceno.11	center		7.96±0.1	8.07±0.1	7.93±0.1	7.93±0.1	7.93±0.05
	right		8.07±0.05	8.18±0.05	7.96±0.14	8.11±0	8.04±0.14
	left		8.11±0.18	8.15±0.05	7.96±0.14	7.96±0.14	8.15±0.29

From table 4.2, the mean of chemical shift artifact distance are not clearly related to echo train length.

### B. Variation of Echo time

The result of the average from scanning three times in echo time when compare in the same echo train length and flip angle is shown in the table 4.3

**Table 4.3** The mean of chemical shift artifact distance when compared echo time 82, 99, 115 in the same flip angle 120 degree and echo train length 10 per slice.

Flip angle 120 ETL 10					
mean			TE 82	TE 99	TE 115
	slice no.1	center	7.52±0.19	7.85±0.1	8.07±0.05
		right	8.15±0.1	7.96±0.05	8.6±0.05
		left	7.74±0.14	8.22±0.16	8.37±0.29
	slice no.6	center	7.48±0.11	7.85±0.05	8.11±0.09
		right	8.11±0.09	8.26±0.1	8.18±0.05
		left	7.71±0.15	8.33±0	8.15±0.1
	sliceno.11	center	7.96±0.1	7.96±0.05	8.04±0.1
		right	8.07±0.05	8.07±0.05	8.26±0.29
		left	8.11±0.18	8.22±0.32	8.15±0.05

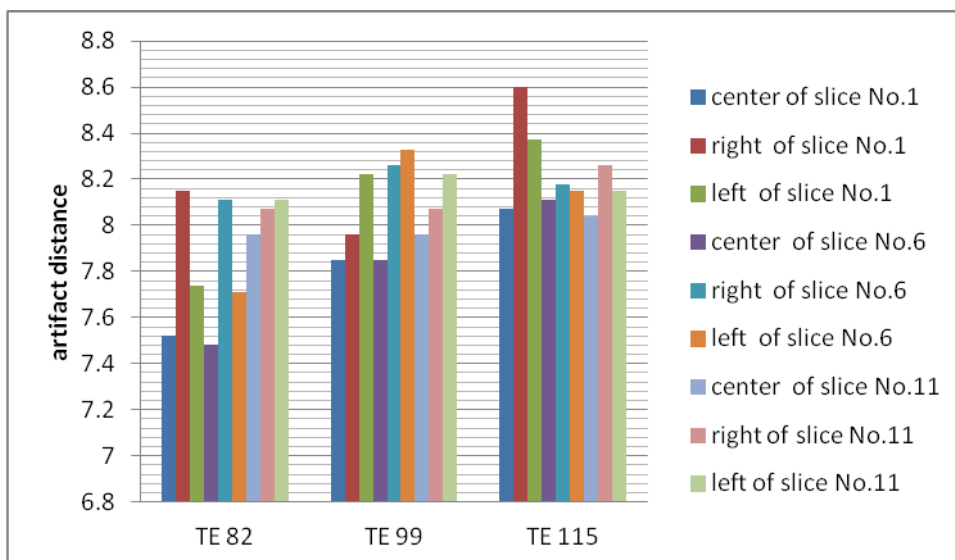


**Figure 4.1** The mean of chemical shift artifact distance when compared echo time 82, 99, 115 in the same flip angle 120 degree and echo train length 10 per slice.

From table 4.4 and figure 4.1, the mean of chemical shift artifact distance were increased when increased echo time.

### C. Variation of Flip angle

The result of the average from scanning three times in flip angle when compare in the same echo time and echo train length is shown in the table 4.8

**Table 4.4** The mean of chemical shift artifact distance when compared flip angle 120, 150,180 degree in the same echo time 82 msec and echo train length 10 per slice.

TE 82 ETL 10					
mean			Flip angle 120	Flip angle 150	Flip angle 180
	slice no.1	center	7.52±0.19	7.26±0.19	6.48±0.14
		right	8.15±0.1	7.82±0.05	7.29±0.05
		left	7.74±0.14	7.33±0.09	7.29±0.14
	slice no.6	center	7.48±0.11	7.15±0.14	5.78±0.09
		right	8.11±0.09	7.45±0.16	6.93±0.05
		left	7.71±0.15	7.41±0.28	7.26±0.23
	sliceno.11	center	7.96±0.1	7.29±0.05	6.96±0.14
		right	8.07±0.05	7.59±0.19	7.4±0.05
		left	8.11±0.18	7.85±0.05	7.4±0.05

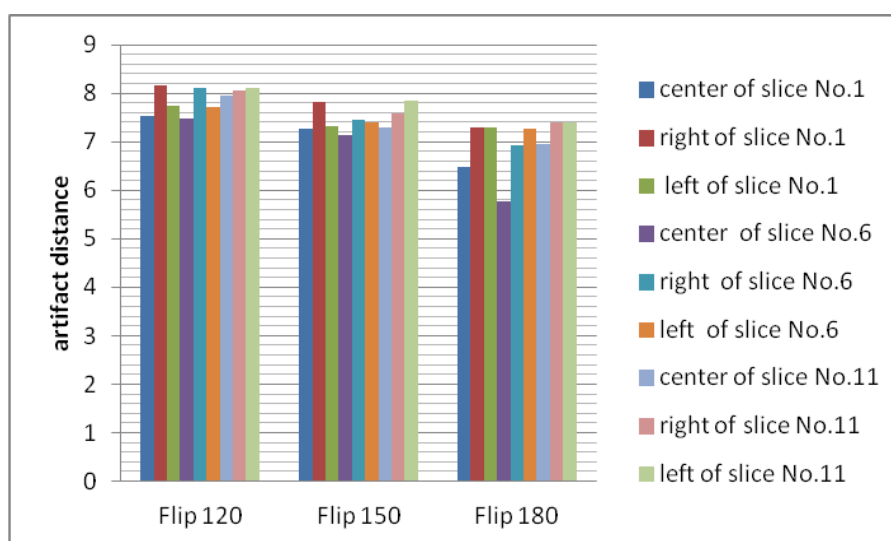


**Figure 4.2** The mean of chemical shift artifact distance when compared flip angle 120, 150,180 degree in the same echo time 82 msec and echo train length 10 per slice.

From table 4.4 and figure 4.2, the mean of chemical shift artifact distance were decreased when increased flip angle.

### D. Variation of difference slices number and position of artifact in the image.

The result of the mean distance from scanning three times when measured in different slice number and different position of artifact in the image by scanning parameter, the same echo time, echo train length and flip angle is shown in figure 4.3

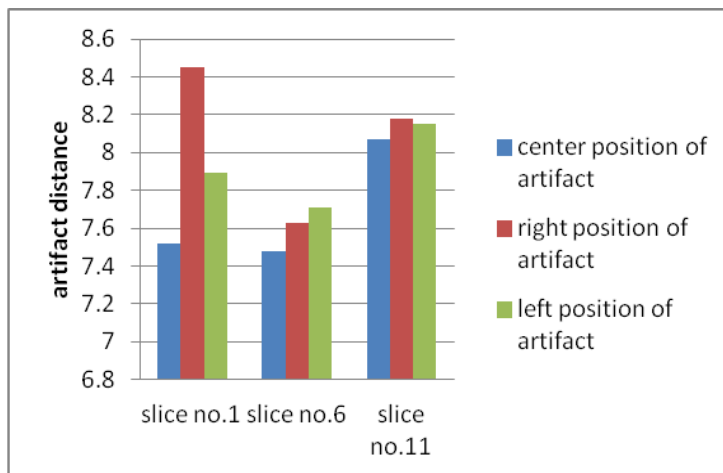


**Figure 4.3** The mean of chemical shift artifact distance when compared slice number 1, 6 and 11 in the same echo time, echo train length and flip angle.

From figure 4.3, the mean of chemical shift artifact distance in slice number 6 was the least and center position of artifact also shown the least.

## CHAPTER V DISCUSSION AND CONCLUSION

### 5.1 Discussion

Although artifacts may be occurred in MRI image but it can be resolved or reduced by optimizing some parameter of MRI scanning. Chemical shift artifact increased when increasing magnetic field strength and decreased when increasing bandwidth. However, magnetic field strength and bandwidth were controlled in this in vitro study using vegetable oil and water filled in the phantom. Chemical shift artifact distances were measured and found increased when echo time increased but decreased when flip angle increased.

#### 5.1.1 Assessment of chemical shift artifact in Echo time (TE).

Chemical shift artifact increased from heterogeneity magnetic field. Reducing Echo time resulted in reduced artifact distance because heterogeneity of magnetic field was also reduced [7]. Echo time is one of the key parameters for establishing T2 or T2\* weighted imaging and creation image contrast [4].

In this study, decreasing echo time results in reduction chemical shift artifact, when fix other scanning parameter.

Therefore, reducing echo time can reduce chemical shift artifact as shown in figure 5.1.

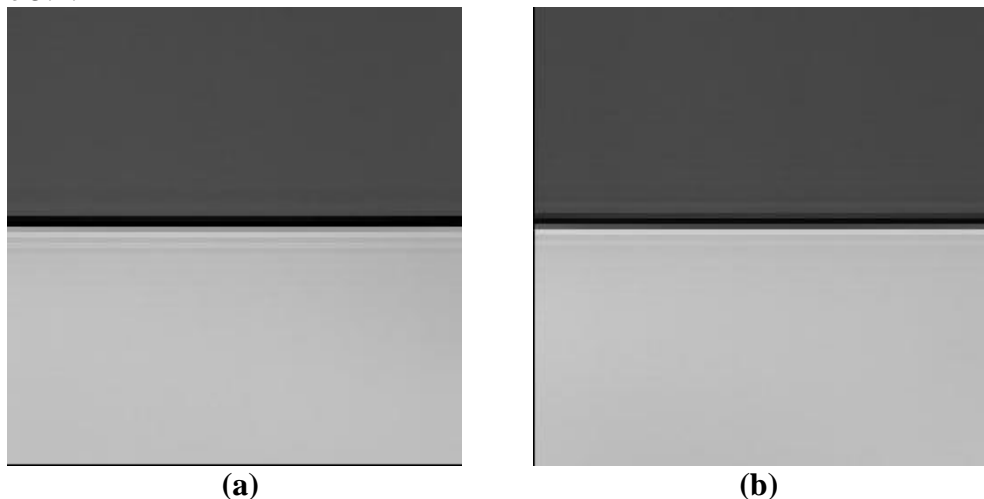


**Figure 5.1** Chemical shift artifact was compared between echo time 82 msec (a) and 115 (b) msec when fixed other scanning parameters.

#### 5.1.2 Assessment of chemical shift artifact in Flip angle.

Chemical shift artifact decreased when increased flip angle. 180 degree. Flip angle in the basis of spin echo pulse sequence is the best chemical shift artifact reduction because spin echo pulse sequence had 180 RF pulses rephrasing to reduce inhomogeneity magnetic field. The flip angle is also a factor in the determination of image contrast for long TR sequences. However, flip angle 180 degree resulted in high specific absorption rate (SAR).

In this study: Increasing flip angle is the result of reduction chemical shift artifact when fix other scanning parameters.

Therefore, increasing flip angle can reduce chemical shift artifact. 180 degree flip angle was the best chemical shift artifact reduction as shown in figure 5.2.

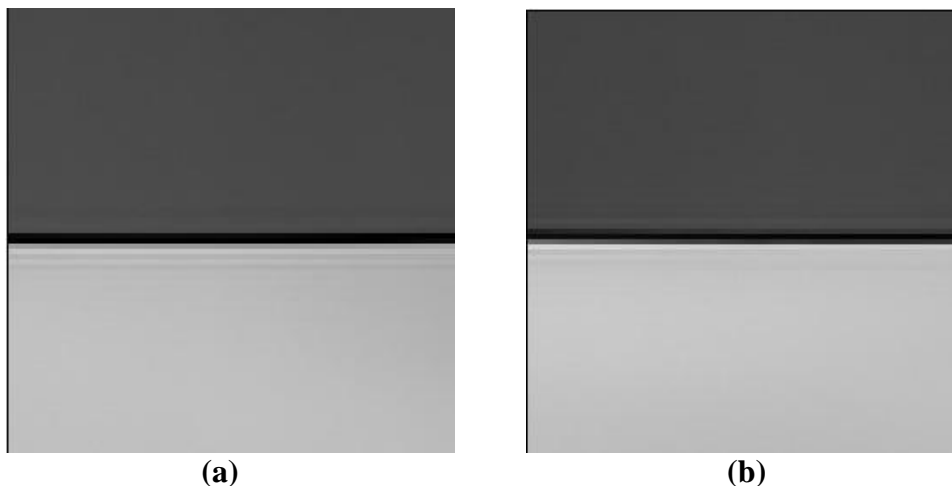
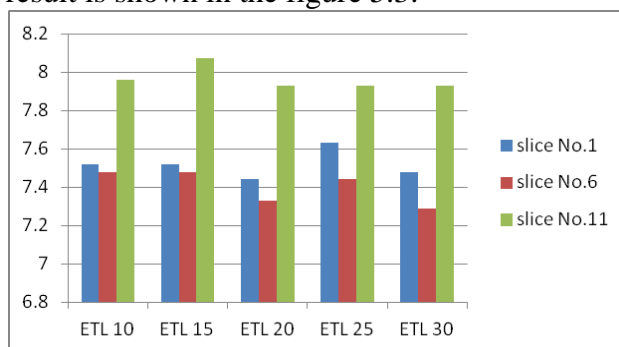


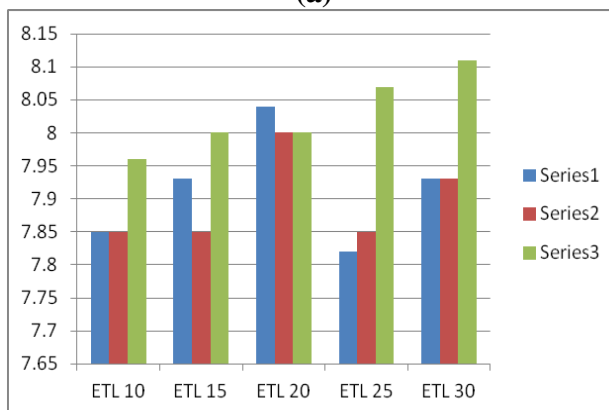
**Figure 5.2** Chemical shift artifact at flip angle 120 degree (a) and 180 degree (b) when fixed other scanning parameters.

**5.1.3 Assessment of chemical shift artifact in echo train length**

Chemical shift artifact distances are not related to echo train length. In this study the echo train lengths were 10, 15, 20, 25 and 30 per slice does not affect clearly due to the range of echo train length in this study were narrow. . However large echo train lengths with short TE result in blurring and loss of contrast that cause chemical shift artifact distance increase. Additional study should be required. Uncertainty of the result is shown in the figure 5.3.



**(a)**



**(b)**

**Figure 5.3** Chemical shift artifact in echo train length 10, 15, 20, 25 and 30 per slice, flip angle 120 when echo time 82 msec (a) and echo time 115 msec (b)

#### **5.1.4 Assessment of chemical shift artifact in different slice number and position of artifact in the image.**

Slice number 6 was shown the least chemical shift artifact distance and center position of artifact in the image also were shown the least due to inhomogeneity magnetic field from distance of isocenter of flux static magnetic field.

#### **5.2 Study limitation**

This study limitation includes unrequired echo time for experiment, filling vegetable oil and water into the acrylic phantom with bubble inside the phantom, surface tension occurred in water and vegetable oil interface that cause difficult measurement chemical shift artifact distance, set position of acrylic phantom before scanning, vibration of both liquid while scanning, uncontrolled signal to noise ratio and specific absorption rate.

#### **5.3 Conclusions**

Decreasing echo time and increasing flip angle result in reduction chemical shift artifact. Slice number 6 and center position of artifact in the image showed the least chemical shift artifact distance. Echo train length is not clearly related to the chemical shift artifact distance.



## REFERENCES

- [1] Liney, P.L. Magnetic Resonance Imaging (MRI).The University of Hull. [Online].2005  
Available from: [www.hull.ac.uk/mri/lectures/gpl\\_page.html](http://www.hull.ac.uk/mri/lectures/gpl_page.html)
- [2] Donald, W.M., Moor, E.A., Graves, M.J., and Prince, M.R. MRI from picture to proton. Cambridge: The United Kingdom at the University Press, 2004.
- [3] Perry sprawls. Magnetic resonance imaging. Spatial Characteristic of the Magnetic resonance Image: Unitate State of America:(2000):89-122.
- [4] Imaging parameters for MRI and protocols for MRI and CT  
available from [www.Commondataelements.ninds.nih.gov/](http://www.Commondataelements.ninds.nih.gov/)
- [5] Robert C. Smith, MD Robert C. Lange, PhD ,et al.Chemical Shift Artifact : Dependence on Shape and Orientation of the Lipid-Water Interface. Radiology 18 (1991):225-229
- [6] Kalevi P. Soila, M.D, et al . Chemical Shift Misregistration Effect in Magnetic Resonance Imaging Radiology 153(1984): 819-820.
- [7] Kampangtip A., Krisanachinda A., Singhara Na Ayudya S. (2012) Technical assessment of artifact production from endo vascular coil at 3 Tesla MRI an in vitro study.6<sup>th</sup> Annual Scientific Meeting, Phitsanulok, Thailand
- [8] American College of Radiology. Magnetic Resonance Imaging (MRI) Quality Control Manual. Reston. VA (2008).
- [9] American Association of Physicists in Medicine. Acceptance Testing and Quality Assurance Procedures for Magnetic Resonance Imaging Facilities. College Park, MD (2010).

## **Appendices**

## Appendix A Case record form

**Distance (mm.) of artifact in the oil and water interface.**

		Distance of artifact in the oil and water interface T2 weighted images TSE.(Flip angle 120°)														
		TE	100 mSec					120 mSec					150 mSec			
Position	ETL slice No.	10	15	20	25	30	10	15	20	25	30	10	15	20	25	30
	Center	1														
11																
16																
Right	1															
	11															
	16															
Left	1															
	11															
	16															



## Appendix B Quality control of MRI systems

**Site:** : Paolo memorial Hospital      **Date:** : 18/06/2012

**Serial Number:** 38271

**Equipment:**

**MRI System Manufacturer:** Siemens Medical System

**Model:** Magnetom Essenza 1.5 Tesla

**Processor Manufacturer:** Intel(R)

**Model:** Syngo MR C13

**QC Phantom: ACR Phantom**

Serial number: J10477

Made in U.S.A

**Determination of seven aspects of image quality**

- Geometric accuracy
- High-contrast spatial resolution
- Slice thickness accuracy
- Slice position accuracy
- Image intensity uniformity
- Percent-signal ghosting
- Low-contrast object detectability

**Procedures the QC Phantom**

Place the QC phantom on the phantom holder with head coil, and level it. Turn the knob facing the cradle to tilt the top of the phantom away from the gantry. Use the laser alignment lights to position the phantom:

The MRI accreditation program requires the acquisition of a sagittal localizer and four axial series of images. The same set of eleven slice locations within the phantom is acquired in each of the four axial series. These images are acquired using the scanner's head coil. The scan parameters for the localizer and the first two axial series of images are fully prescribed by the ACR in the scanning instructions as the **ACR sequence** or **ACR images**. The third and fourth series of axial images are based on Paolo Memorial Hospital is the Spin echo T1 and T2 protocols and are referred to as the set sequences or site images. To discuss the image data it is convenient to introduce names for the different sets of image and numbering for the slice locations within the phantom.

The localizer is a 20 mm thick single slice spin echo acquisition through the center of the phantom, and is referred to simply as the **localizer**.

The first axial series is a spin echo acquisition with ACR specified scan parameters that are typical of T1-weighted acquisitions. This series is called the ACR T1 series.

The second axial series is a double spin echo acquisition with ACR specified scan parameters that are typical of proton density/T2-weighted acquisitions. When

analyzing data from this acquisition, only the second-echo image is used. The set of second-echo image from this acquisition is called the ACR T2 series.

The third and fourth axial series re based on the scan parameter at Paolo Memorial Hospital normally uses in its clinical protocols for axial head T1 and T2 weighting respectively. These series are called the site T1 and site T2 series.

For all four axial series the required slice thickness is 5 mm and the slice gap is 5mm thus, the set of eleven slice spans a distance of 100 mm from the center of the first slice to the center of the last slice.

### Pulse Sequence Acquisition Parameters

**Table 1** ACR Pulse sequence acquisition parameters.

Study	Pulse Sequence	TR (ms)	TE (ms)	FOV (cm)	No of Slices	Slice Thick. (mm)	Slice Gap (mm)	NEX	Matrix		Band Width (kHz)	Scan time (min.sec)
ACR Sagittal locator	Spin echo	400	10	25	1	20	20	1	256	256	2.06	0.59
ACR Axial T1	Spin echo	500	20	25	11	5	5	1	256	256	82.06	1.01
ACR Axial T2	Spin echo	2000	80	25	11	5	5	1	256	256	82.06	1.05

**Table 2** Clinical protocols: Pulse sequence acquisition parameters.

Study	Pulse Sequence	TR (ms)	TE (ms)	FOV (cm)	No of Slices	Slice Thick. (mm)	Slice Gap (mm)	NEX	Matrix		Band Width (kHz)	Scan time (min.sec)
ACR Axial T1	Gradient echo	150	2.3	24	11	5	5	1	256	256	173.60	1.14
ACR Axial T2	Spin echo	4000	70	24	11	5	5	1	256	256	275.15	1.15

## 1. Geometric Accuracy

**Purpose:** To assess the accuracy which the image represents lengths in the geometric test. A failure means that dimensions in the images differ from the true dimensions substantially more than +- 2mm.

**Method:** Display the image localizer, slice 1 of the ACR T1 series, and slice 5 ACR T1 series. Seven measurements the diameters of the phantom of known lengths within the phantom are made using the display station on screen length measurement tool.

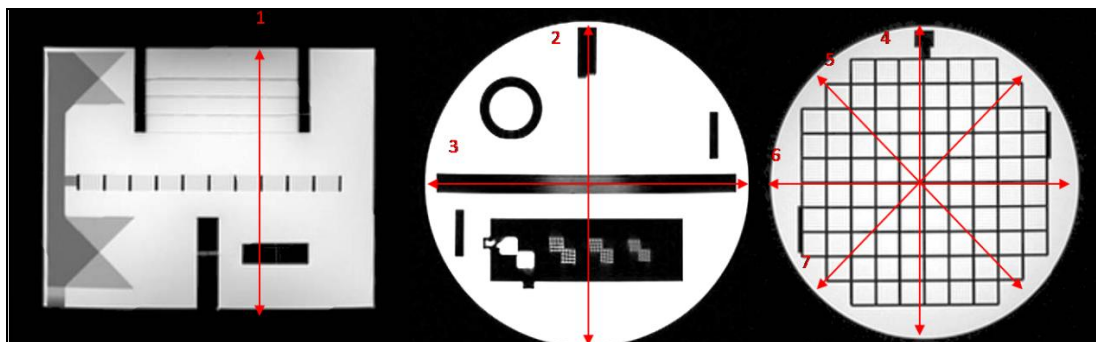


Figure A 1 Geometric accuracy

Table 3 Result geometric accuracy

Line No.	True Value (mm)	Sag Locator		ACR T1		ACR T2	
		Meas. (mm)	Diff (mm)	Meas. (mm)	Diff (mm)	Meas. (mm)	Diff (mm)
1	148	147.77	-0.23	-	-	-	-
2	190	-	-	190.1	0.1	190.6	0.6
3	190	-	-	190.6	0.6	190	0
4	190	-	-	191.4	1.4	190.6	0.6
5	190	-	-	189.2	-0.8	189.8	-0.2
6	190	-	-	189.6	-0.4	189.6	-0.4
7	190	-	-	191.0	1	189.4	-0.6

**Recommended Action Criteria:** +/- 2 mm in all planes.

**All are:** Pass

## 2. High Contrast Spatial Resolution

**Purpose:** To test the scanner's ability to resolve small objects when the contrast to noise ratio is sufficiently high. A failure of this test means that for given field of view and acquisition matrix size the scanner is not resolving small details at 1.0mm.

**Method:** Display the slice 1 ACR axial series, magnify the image by factor of between 2 and 4, look at the rows of holes in the UL (Upper left) arrays and adjust the display windows and level to best show the holes as distinct from one another. If all four holes in any single row are distinguishable from one another, score the image as resolved right to left at this particular hole size. Look at the hole in the LR (Lower right) array and adjust the display window and level to best show the holes as distinct from one another. Make a note of the smallest hole size resolved in each direction; that is the measured resolution for that direction.



Figure A2 ACR protocol



**Figure A3** Clinical protocols

**Table 4** Result high contrast spatial resolution

	<b>Spatial Resolution</b>	<b>Result</b>
ACR Axial T1	>0.9 mm	Pass
ACR Axial T2	>0.9 mm	Pass
Clinical Axial T1	0.9 mm	Pass
Clinical Axial T2	0.9 mm	Pass

**Recommended Action Criteria:** 1 mm or larger

### 3. Image intensity Uniformity: Percent integral Uniformity (PIU)

**Purpose:** To measure the uniformity of the image intensity over a water region of the phantom lying near the middle of the head coil. Head coils for clinical use have fairly uniform spatial sensitivity near the middle of the coil when loaded as typical for a human head. Failure of this test means that the scanner has significantly greater variation in image intensity than 12.5 percent. Lack of image intensity uniformity indicates a deficiency in the scanner, often a defective head coil or problem in the radio frequency subsystems.

**Method:** Display slice location 7. Place a large, circular region of interest on image. This ROI should have an area between 195 and 205 cm<sup>2</sup>. Set the display window to its minimum, and lower the level until the entire area inside the large ROI is white. Place a small ROI roughly 1 cm<sup>2</sup> at the region of dark pixels inside the large ROI. Record the mean pixel value for this 1 cm<sup>2</sup> ROI. This is the measured low signal value. Now raise the level until all but a small, roughly 1 cm<sup>2</sup> region of white pixels remains inside the large ROI. This is the region of highest signal. Record the average pixel value for this 1 cm<sup>2</sup> ROI. This is the measured high signal value.

The measured high and low signal values for each of the ACR series are combined to produce a value called **percent integral uniformity (PIU)**. Use the following formula to calculate PIU: **PIU = 100x (1 - {(high-low)/(high+low)})**.

**Table 5** Result Image intensity uniformity

	<b>Low signal</b>	<b>High signal</b>	<b>PIU</b>	<b>Result</b>
ACR Axial T1	1840.4	2006.8	95.67	Pass
ACR Axial T2	1193.9	1317.0	95.1	Pass

**Recommended Action Criteria:** PIU should be greater than or equal to 87.5% for MRI systems with field strengths less than 3 Tesla.

### 4. Percent-signal ghosting



**Purpose:** To assess the level of ghosting in the image. Ghosts are most noticeable in the background areas of an image where there should be no signal, but usually they overlay the main portions of the image as well, artifact actually altering the image intensities. A failure of this test means that there is signal ghosting at a level significantly higher than that observed in a properly functioning scanner.

**Method:** Percent signal ghosting measurement is made on slice 7 of the ACR T1 series. Using the workstation's ROI tool, five intensity measurements are made: the average intensity in the primary image of the phantom, and the average intensity of the background at four locations outside of the phantom. The value for the ghosting as a fraction of the primary signal is calculated using the following formula.

$$\text{Ghosting ratio} = \frac{((\text{top} + \text{btm}) - (\text{left} + \text{right}))}{(2 \times (\text{large ROI}))}$$

Where top, btm, left, right and large ROI are the average pixel values for the ROIs of the same names. The vertical bars enclosing the right hand side of the equation mean to take the magnitude of the enclosed value.

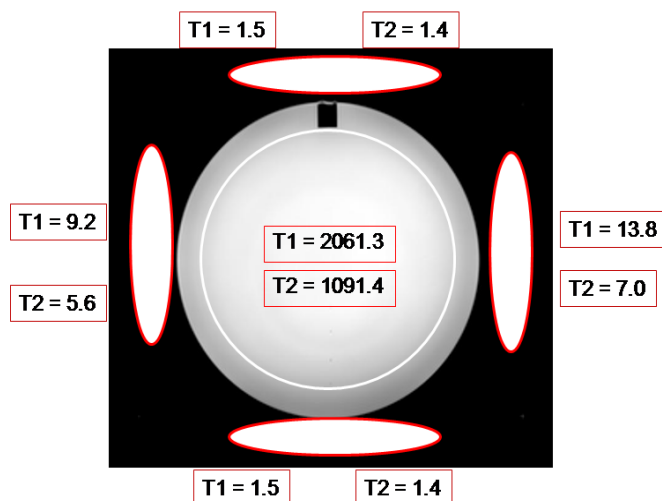


**Figure A4** Percent signal ghosting

**Table 6** Pixel Value

	T1	T2
Large ROI	2061.3	1091.4
Lt.ROI	59.2	5.6
Rt.ROI	13.8	7.0
TOP ROI	1.5	1.4
Bottom ROI	1.5	1.4

**Table 7** Result Percent signal ghosting

	Ghosting Ratio	Result
ACR Axial T1	0.0014	Pass
ACR Axial T2	0.0072	Pass

**Recommended Action Criteria:** The ghosting ratio is less than or equal to 0.025.

## 5. Low Contrast Object Detectability

**Purpose:** To assess the extent to which object of low contrast are discernible in the images. The ability to detect low contrast objects is primarily determined by the

contrast to noise ratio achieved in the image, and may be degraded by the presence of artifact such as ghosting. A failure of this test means the images produced by the scanner show significantly fewer low contrast objects than most properly functioning clinical scanner.

**Method:** Measurements are made for the ACR and clinical series. The low contrast objects appear on four slices: slice 8 through 11. In each slice the low contrast objects appear as rows of small disks, with the rows radiating from the center of a circle like spokes in a wheel. Each spoke is made up of three disks, and there are ten spokes in each circle. All the disks on a given slice have the same level of contrast. In order from slice 8 to slice 11, the contrast value are 1.4%, 2.5%, 3.6%, and 5.1%. All the disks in a given spoke have the same diameter. Starting at the 12 o'clock position and moving clockwise, the disk diameter decreases progressively from 7.0mm at the first spoke to 1.5 mm at the tenth spoke. The measurements for this test consist of counting the number of complete spokes seen in each of the four slices. This is done for each of the four axial series.

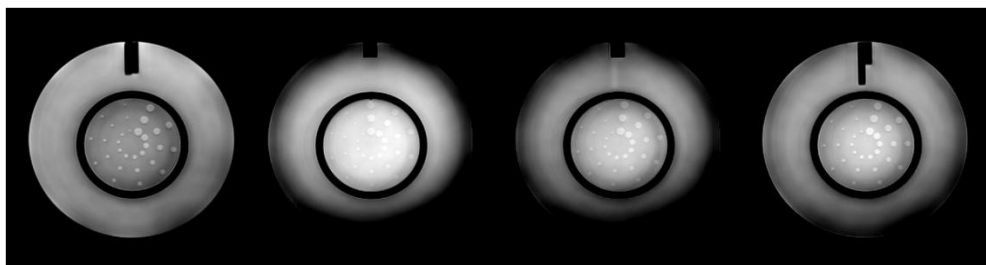


**Figure.5** T1 low contrast object detectability

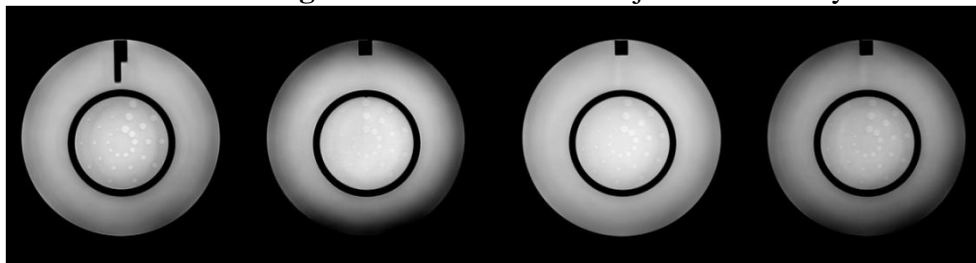


**Figure.6** T2 low contrast object detectability

**Table 7** Result low contrast object detectability

Contrast Value	Number of Spoke				Total	Result
	1.40%	2.50%	3.60%	5.10%		
ACR Axial T1	9	10	10	10	39	Pass
ACR Axial T2	6	10	10	10	36	Pass

**Recommended Action Criteria:** A total score of at least 9 spokes for MRI systems with field strengths less than 3 Tesla is accepted.

## 6. Slice Position accuracy

**Purpose:** To assess the accuracy with which slices can be prescribed at specific locations utilizing the localizer image for positional reference.

**Method:** Slice position accuracy test the differences between the prescribed and actual positions of slices 1 and 11 are measured. These measurements are made for the ACR T1 and T2 series. The Slice 1 and 11 are prescribed so as to be aligned with

the verticals of the crossed 45° wedges at the inferior and superior ends of the phantom respectively. On slice 1 and 11 the crossed wedges appear as a pair of adjacent, dark, vertical bars at the top of the phantom. For both slice 1 and slice 11, if the slice is exactly aligned with the vertex of the crossed wedges, then the wedges will appear as dark bars of equal length on the image. By design of the wedges, if the slice is displaced superiorly with respect to the vertex, the bar on the observer’s right will be longer. If the slice is displaced inferiorly with respect to the vertex, the bar on the left will be longer.

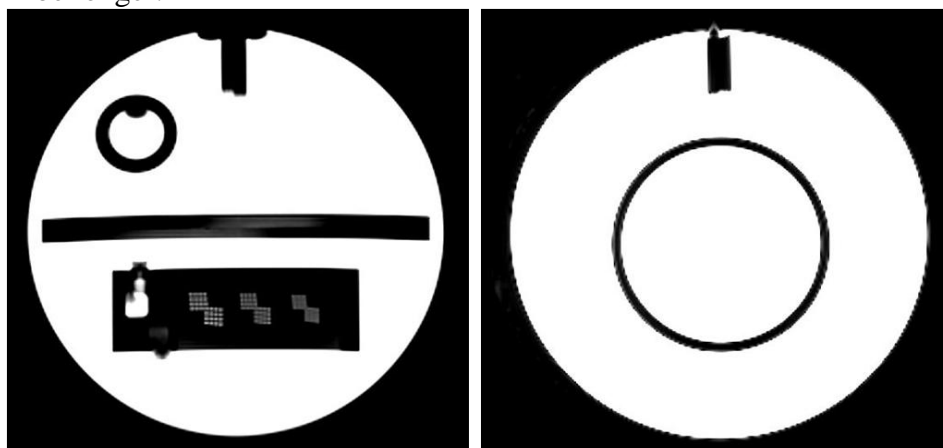


**Figure A7** Slice position accuracy

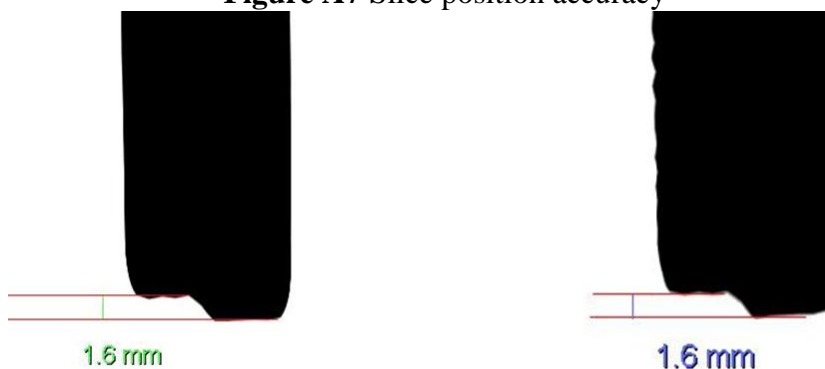


**Figure A8** Slice position accuracy

**From slice Position 1 and 11 ACR Phantom:**

Wedge (mm)	= +	= -	
	<b>T1</b>	<b>T2</b>	
Slice Location: 1	0.13 mm	0.14 mm	<b>Pass</b>
Slice Location: 11	0.3 mm	0.32 mm	<b>Pass</b>

**Recommended Action Criteria:** The magnitude of each bar length difference should be less than or equal to 5 mm.

## 7. Slice Thickness Accuracy

**Purpose:** To assess the accuracy with which a slice of specified thickness is achieved. The prescribed slice thickness is compared with the measured slice thickness. A failure of this test means that the scanner is producing slices of substantially different thickness from that being prescribed. This problem would rarely if ever occur in isolation since the scanner deficiencies that can because it will also cause other image problems. Therefore, the implications of a failure are not just that the slice are too thick or thin, but can extend to things such as incorrect image contrast and low signal to noise ratio.

**Method:** Slice thickness accuracy test the lengths of two signal ramp in slice 1 are measured. This is done for both ACR series. The ramps appear in a structure called the slice thickness insert. The two ramps are crossed: one has a negative slope and the other a positive slope with respect to the plane of slice 1. They are produced by cutting 1 mm wide slots in a block of plastic. The slots are open to the interior of the phantom and are filled with the same solution that fills the bulk of the phantom. The signal ramps have a slope of 10 to 1 with respect to the plane of slice 1, that is they make an angle of about  $5.71^\circ$  with slice 1. Therefore, the signal ramp will appear in the image of slice 1 with a length that is 10 times the thickness of the slice if the phantom is tilted in the right-left direction, one ramp will appear longer than the other. Having crossed ramps allows for correction of the error introduced by right-left tilt.

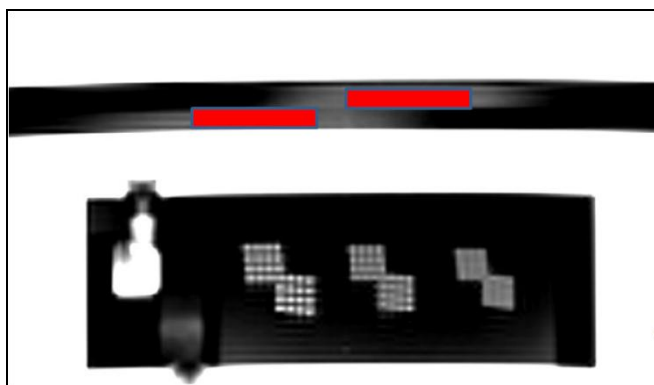


**Figure A8** Magnified region of slice 1 showing slice thickness signal ramps with ROIs placed for measuring average signal in the ramps.

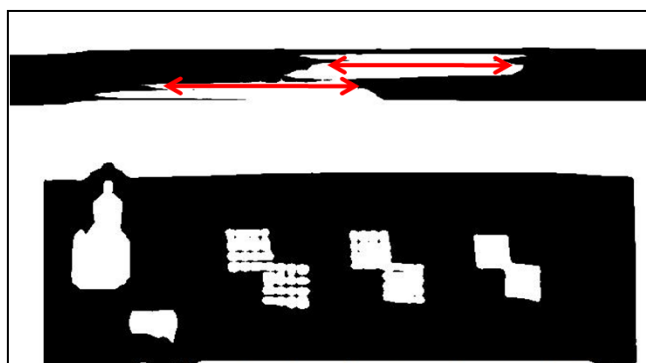


**Figure A9** Magnified region of slice 1 showing slice thickness signal ramps. The display window is zero and level is half the average signal level of the ramps. The length measurement for the ramps are shown on the image

**From Slice Position: 1 of the ACR Phantom:**

The slice thickness is calculated using the following formula

$$\text{Slice thickness} = 0.2x (\text{top} \times \text{bottom}) / (\text{top} + \text{bottom})$$

The length at signal ramps between top and bottom are measured.

**Table 8** Result slices thickness accuracy.

Series	Slice Thickness Set (mm)	Slice Thickness Measured (mm)	Results
Brain T1	5 mm	5.7 mm	Pass
Brain T2	5 mm	5.13mm	Pass

Slice Thickness      Top: 44.9      Calculate slice  
                                  Bottom: 53.7      (FWHM in mm) Thicknesses (mm): 4.8

**Recommended Action Criteria:** For both ACR series the measured slice thickness should be 5.0 mm+- 0.7 mm.

**8. Magnetic Field Homogeneity**

Method Used (Spectral peak): Spectral Peak 63.65 Hz

Measured Homogeneity: cylinder volume (cm<sup>3</sup>): 40x40x30

Homogeneity (ppm): 0.1

**VITAE**

<b>Name</b>	Mr. Nuttapong Danthanavat
<b>Date of birth</b>	September 3, 1984
<b>Place of birth</b>	Bangkok, Thailand
<b>Education</b>	Bachelor of Science in Radiological Technology program Faculty of Medical Technology Mahidol University, 2008
<b>Work Experiences</b>	2009-Present Radiological Technologist, Department of radiology, Paolo memorial Hospital, Bangkok
<b>Address</b>	5 Vibhavadi Rangsit Road Din Daeng, Bangkok, Thailand